**Title**
Current Aperture III-Nitride Edge-emitting Blue Laser Diode



**Author**
Megalini, Ludovico

**Publication Date**
2014

UNIVERSITY OF CALIFORNIA

Santa Barbara

# Current Aperture III-Nitride Edge-emitting Blue Laser Diode

A Thesis submitted in partial satisfaction of the

requirements for the degree Master of Science

in Electrical Engineering

by

Ludovico Megalini

Committee in charge:

Professor Steven P. DenBaars, Chair

Professor John. E. Bowers

Professor Shuji Nakamura

Dr. Daniel A. Cohen

June 2013

The thesis of Ludovico Megalini is approved.

John E. Bowers

Shuji Nakamura

Daniel A. Cohen

Steven P. DenBaars, Committee Chair

March 2013

Current Aperture III-Nitride Edge-emitting Blue Laser Diode

*“La fatica non è mai sprecata. Soffri ma sogni”*

Pietro Mennea,
Campione Olimpico e Mondiale

*“Sweating the hard stuff is never wasted.
You suffer but in the meantime you dream”*

Pietro Mennea,
Olympic and World Champion

To my late father Domenico,

my mum Giovanna and my sister Mariarosaria

## ACKNOWLEDGEMENTS

On a sunny morning of July of about four years ago, while I was getting bored at doing some data entries relative to some financial operations done who knows where, my mobile rang. The number was partially hidden and I was a little hesitant to answer: after all I was bored enough to listen also to any whatever summer ads. Finally, I decided and from the other side a voice said: <<Mr. Megalini? I am from the Fulbright Commission in Rome and I am glad to announce you are the winner of the Fulbright-Finmeccanica scholarship for this year>>. Considering that I had graduated since more than three years ago, do you think that this may even be possible? No?? Well, you are wrong. To be honest, at the beginning I also thought it was a joke and I was going to shut down but after I looked better at the mobile number, +39-06-xxxxx, and I realized that the phone call was indeed coming from Rome, I started to believe that a dream could have become reality. Indeed, about a year later (and a broken engagement), the day 67 year after the proclamation of the armistice between Italy and the USA (and all the Allies) I was flying over the Atlantic ocean to start this new adventure. Following the suggestion of Prof. B. Wardle, my master thesis project advisor at MIT, and a short talk to Prof. Banerjee, whose contact was given to me by Prof. Ionescu after I took a good grade on his class about nanoelectronics at the EPFL, I decided to go to UCSB.

To be honest, initially I was not totally convinced of my choice.

At that time, the only things that I knew about UCSB were its location in a wonderful place (absolutely true!) and the many parties which were organized essentially every day; moreover I had also been admitted to some other US universities, and one of these had even offered the possibility of getting both a MSc in Engineering and a MA in Economics plus an additional scholarship on top of the Fulbright (which by the way was not enough to cover the tuitions and fees for an academic year at UCSB). Now that I have completed the MSc program and, most of

all, now that I am a PhD candidate in one of the best Materials department of the world, I can say that that choice was probably the right one.

A MSc. thesis is not a PhD thesis and as a consequence of this self-evident statement worth of Monsieur La Palisse, one would expect to read a short page of acknowledgments. For many different reasons, this is not the case of this work. As I mentioned before, my first and foremost thanks goes to the Italy-US Fulbright Commission. I want to stress again the fact that they really made a dream to become a reality. I had already been to the US in 2007 as exchange student at MIT for a semester but what the Fulbright Commission has offered to me was a totally new challenge. I feel I can never thank it enough. In particular, Dr. Barbara Pizzella has been very kind in assisting me in filing all the required documents and incredibly patient in answering to all my doubts and questions. Carlo Musso of Finmeccanica, the company which has co-sponsored my scholarship was also available when necessary.

On the US side, I am extremely grateful to my PhD advisor Prof. Steven P. DenBaars.

He has been for me like a second Fulbright Commission and I am trying my best to meet his expectative by the end of my PhD.

Not only he has allowed me to finish the MSc program but more importantly he has accepted me to do a PhD in his group, despite he has every day a similar request by hundreds of American, Chinese and Korean students coming from the most prestigious American and world universities, despite I did not have any supporting scholarship for the following years in a time when all the universities are struggling to look for funding (and moreover being an international student I am very expensive), despite I would have started my PhD at an age when the PhD students of his group were in general going to graduate. The fact that he is successful manager, apart from being a MOCVD world expert and having set up a great MOCVD lab, is definitely something to mention.

I want to thank also the other members of my Committee: Prof. J. Bowers and Prof. Nakamura. I am looking forward to receiving from them more precious inputs and collaborate with their groups.

Dr. Dan Cohen is not just another member of this Committee to thank. He has been the deus-ex-machina of this project, the person which has been always available to talk for advice about processing, explanations of theory, setting up the measurements tests and so on. I wish I will have the opportunity to keep on working with him for the rest of my PhD and hopefully by then he will not get too annoyed by my thousands of questions.

Val De Veyra has been instrumental in helping me with the bureaucracy since the very first time and throughout all this time in the ECE Dept. I did enjoy our conversations in Ital-english about Italian food and Montalbano and I am sure we will have many more. In the Materials Dept. I need to thank Sheryl, Tara, Alison, Oura and Yukina for their assistance with administrative issues. This works is mainly focused on PEC-etching and will continue with laser so I want to thank all the laser team for the useful discussion, in particular Dan Hager, Shih-Chieh (Walsin), Kate Kelchner and Bob Farrell have been of precious help. When I joined Prof. DenBaars group, I got also a lot of help from some LED guys, in particular Nathan Pfaff, Eddie Pan and Jason Jewell, which has been also a great roommate and probably the best American friend I met in Santa Barbara. Great roommates during my first year in San Clemente have also been Miguel, Tony and Edy. Deblina, Eddie Pan and Elizabeth Rangel provided me some useful courses materials. Sean Demura has been very kind in teaching me how to use several cleanroom tools. Thanks to Asako Hirao for the summer internship I spent at OSRAM, it was a great experience. I had a lot of fun time with many Italian that I met at UCSB, especially Paolo A., Paolo G., Stefano, Misael, Alessandro, Mirko, Paolo P. and Pietro. I feel I have also to thank Nicole, Jennifer and especially Yuri. Finally I do want to thank my family, my late father Domenico, my mother Giovanna and my sister Mariarosaria.

ABSTRACT

Current Aperture III-Nitride Edge-emitting Blue Laser Diode

by

Ludovico Megalini

This work presents the first Nitride non polar Current Aperture Edge Emitting Blue Laser Diode (CA-LD) fabricated using the Photo-Electro-Chemical Etching (PECE) technique.

The main features of this design are represented by the deep etching of the laser diode ridge through the active region, the controlled etching of the active region by PECE and the increase of the p-contact area with respect to the active region area. Preliminary experiments manifest that CA-LD has similar threshold current density, slope efficiency and peak output power of the more commonly used shallow etch ridge design and it has also shown a reduction in the series resistance down to ~40% with respect to the shallow-etch LDs indicating the potential of the CA-LD design in high-efficient, high-power, high-frequency LD applications.

TABLE OF CONTENTS

LIST OF FIGURES

LIST OF TABLES

## Introduction

The need to satisfy the constant rising global energy demand in a sustainable way has become a worldwide issue of paramount importance: global warming, economic revival and even national security have indeed forced all the countries of the world to reduce their fossil fuel consumption and dependence in favor of seeking environmentally clean alternative energy resources and energy efficiency[1,2] devices. Future energy demands is projected to increase considerably relative to value of 2001: according to the scenario developed by the Intergovernmental Panel on Climate Change (IPCC), the world energy consumption rate would grow from the average value of 13.5TW in 2001 to ≈40.8TW in 2050 due to population and economic growth[3], even in the face of substantial declines in energy intensity[1].

[1] The scenario is based on moderate assumptions that means "business as usual": neither overly conservative nor overly aggressive.

Among all the highly efficient energy devices, III-Nitride solar cells, LEDs and laser diodes stand out.

Solar energy is by far the largest and more abundant of all the clean renewable energy resources all the clean renewable energy resources one: more energy from sunlight strikes the earth in one hour ($4.3 \cdot 10^{20}$ J) than all of the energy currently consumed on the planet in one year ($4.1 \cdot 10^{20}$ J in 2001). Indeed the sun energy, which comes from thermonuclear reaction, is an abundant, free, and nonpolluting source of energy with multiple possible applications. According to an analysis from McKinsey[4], over the last two decades the cost of manufacturing and installing a solar PV system has decreased by about 20% with every doubling of installed capacity and considering the rising of oil and natural gas prices, the need to build new power plants to keep up with the growing demand and the regulation aiming to limit CO2 emission, it has been esteemed that by ten years electricity generated from solar energy could cost to the end user as much as the one by fossil fuel in some countries[5] such Italy and California, as represented in Fig. 1.

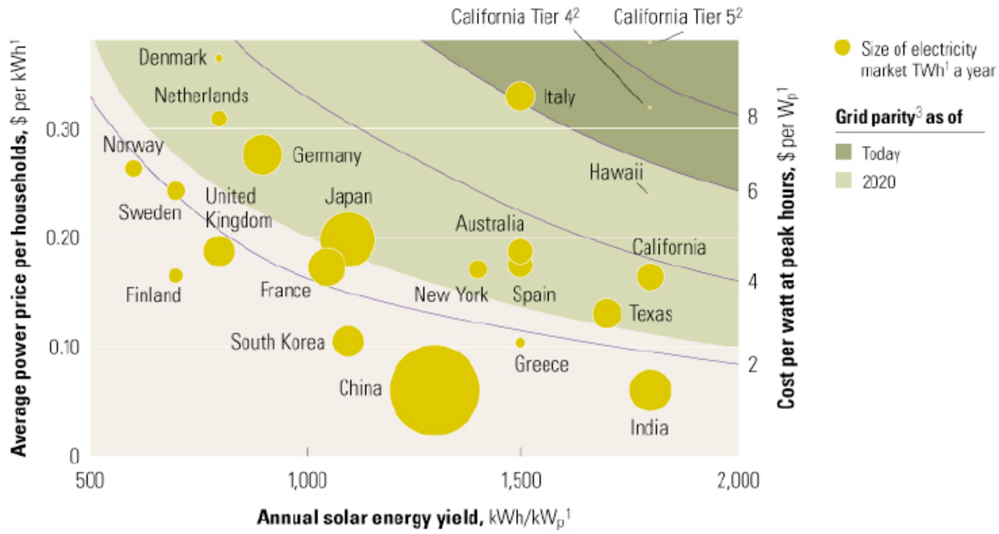


[1]kWh = kilowatt hour; $kW_p$ = kilowatt peak; TWh = terawatt hour; $W_p$ = watt peak; the annual solar yield is the amount of electricity generated by a south-facing 1 kW peak-rated module in 1 year, or the equivalent number of hours that the module operates at peak rating.
[2]Tier 4 and 5 are names of regulated forms of electricity generation and usage.
[3]Unsubsidized cost to end users of solar energy equals cost of conventional electricity.

Source: CIA country files; European Photovoltaic Policy Group; Eurostat; Pacific Gas & Electric (PG&E); Public Policy Institute of New York State; McKinsey Global Institute analysis

**Figure 1 The growing competitiveness of solar power [From 4]**

Although such analysis shows the feasibility of the solar energy as a valid and immediate energy resource, currently only 0.1% of electricity is provided by a solar source and the solar market has been suffering turmoil with big companies having many financial problems and even went to bankrupt[6]. The great challenge is to increase the efficiency of the solar cells and at the same time to reduce the $/W of the materials used to fabricate the panels.

While solar cell play an important role in generating cheap and green energy, nitride solar cells have currently not penetrated the market; on the other hand LEDs and LDs are devices which exploit energy in a very highly efficient way and they both have found a widespread use not only in consumer electronics but they have cornered the biggest and profitable market of the Solid State Lighting.

Since the development of incandescent light bulbs in the late 1800s, various methods of producing light more efficiently have been investigated. Of these, light sources based on light-emitting diodes (LEDs) appear to have a considerable impact on issues such as energy consumption, environment and even the health of individuals[7,8]. Nowadays roughly 22% of the electricity generated in the United States is dedicated to lighting applications and it has been computed that if all conventional white light sources in the world were converted to the energy-efficient LED light sources, energy consumption could be reduced by around 1,000 TWh/yr, the equivalent of about 230 typical 500-MW coal plants, reducing greenhouse gas emission by about 200 million tons. White-light sources based on reliable and energy-efficient LEDs have only recently been made possible[9] and until not so long time ago the only high-luminosity LEDs available emitted red light. In addition there are still several issues in producing white light from GaN based LEDs: in general white light is produced by a yellow- emitting phosphor combined with blue LEDs.

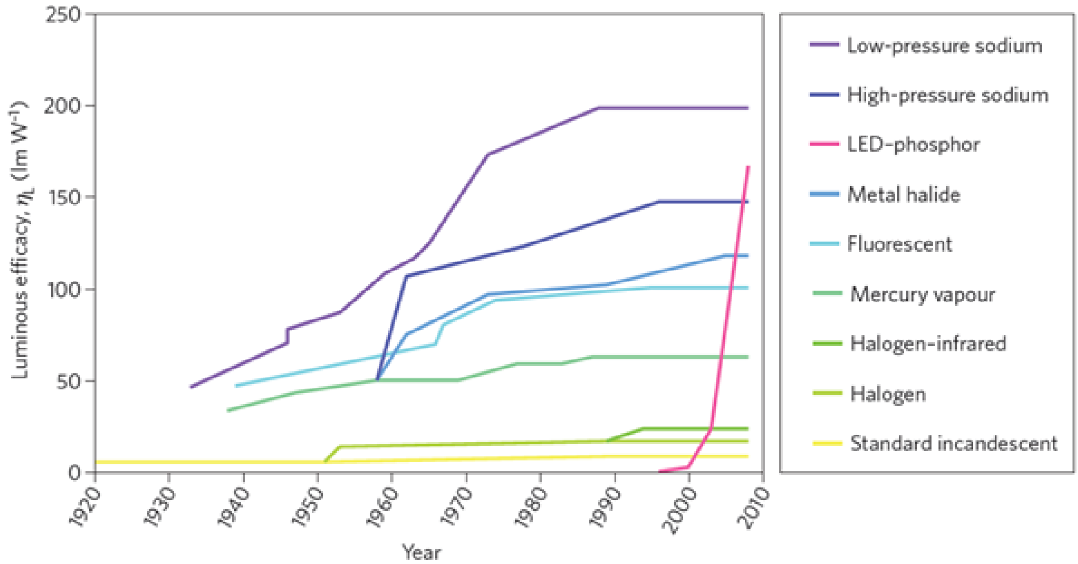


**Figure 2 Historic development of the most common white-light sources [From 7]**

Laser Diodes (LDs) present even more advantages of LEDs: they have entered in widespread use as the laser source in many applications for high-density optical data storage (Blu-ray), medical and biomedical instrumentation, powerful tool to cut paper, etch leather or glass, or brand wood, chemical and biological agent detection to sterilization and advanced lithography. Such a huge variety of applications has been made possible by the flexibility these devices offer in tuning the wavelength and the space power distribution, differently from the case of the gas lamps for which emission wavelength is predetermined by fundamental transitions in gas or vapor. As example, the UV market alone is forecasted to be worth as much as $150 million in 2016 up to 5 times its value in 2011, and even much bigger market would be represented by the pico-projector to be embedded in the mobile phones and in the

TVs. More recently, it has been suggested the use of LDs to replace LEDs in Solid State Lighting applications[10]. Currently, LEDs have a wall plug efficiency4 (wpe) more than twice higher than high performance c-plane blue LDs5 (~70% vs ~30% for LEDs and LD at a low and high input power density respectively). However, LDs may potentially outperform the LEDs because at high input power density (>6kW/cm2) are less affected by the efficiency droop typical of the LEDs, since all the parasitic nonradiative recombination processes are clamped at their lasing threshold values. Moreover, nonpolar/semipolar devices appear promising for higher performance and reliable LDs because of the elimination/mitigation of the intrinsic polarization field, which leads to the increase overlap of the carriers wavefunction, and the gain maximization along some proper crystal plane orientations. However many problems ranging from material growth to device processing remain to be solved.

Photo-Electro-Chemical Etch (PECE) is currently the only viable wet etching technique for the nitride system. As a wet etching technique, it produces a relatively gentle etch and it also offers several advantages, in particular the bandgap selectivity etch which allows more freedom in designing new devices with higher performances. This technique has been used as powerful technique to help solving some of the processing issue and as a result to improve nitride-based device performance, in particular nitride LDs.

## *References*


[1] Hubbert, M. K. “*Energy from Fossil Fuels*”, Science **109**, 103-109, (1949).

[2] Campbell, C. J.; Laherrere, J. H. “*The end of cheap oil*”, Sci. Am., **278**, 60-65, (2008)

[3] N.S.Lewis and D.Nocera, “*Powering the Planet*”, PNAS Vol.103, No. **43**, 24 October 2006, 15729-15735

[4] Lorenz P, Dickon P., Seitz T., “*The economics of solar power*”, The McKinsey Quartely, 10, (2008)

[5] J.F. Kirkegaard, T. Hanemann, L.Weischer,and M. Miller, “*Toward a Sunny Future? Global Integration in the Solar PV Industry*”, Peterson Institute working paper series 10–6, 5, (2010)

[6] http://www.nytimes.com/2011/11/25/opinion/the-solyndra-mess.html

[7] S. Pimputkar, J.S. Speck, S. P. DenBaars and S. Nakamura, “*Prospects for LED lighting*”, Nature photonics, **3**, (2009)

[8] Robert V. Steele, “*The story of a new light source*”, Nature photonics, **1**, (2007)

[9] S. Nakamura and M.Riordan, “*The Dawn of Miniature Green Lasers*”, Scientific American, April, (2009)

[10] J.J. Wierer, J.Y. Tsao, and D.S. Sizov, Laser & Photon. Rev., **7**, 963 (2013)

# Chapter 1

## 1.1 History of Nitride-based LDs

The history of Nitride LDs is indissolubly related to Prof. Nakamura[1].

The first LDs were developed in 1962 on GaAs by Robert N. Hall at the General Electric research center and by Marshall Nathan at the IBM T.J. Watson Research Center, in the same year Nick Holonyak, Jr demonstrated the first LD emitting in the visible range. Continuous-wave (cw) lasing at room temperature was achieved in an AlGaAs/GaAs double-heterostructure laser in 1970. In June 1991 3M released the first ZnSe-CdZnSe based laser. Being the defect density in ZnSe very low, the majority of the groups focused their research efforts on ZnSe and II-VI.

In June 1992 a breakthrough happened: Nakamura, which at that time was working for Nichia, grew a single crystal InGaN layer and in Sept 1992 he built first double hetero-structure based light emitting diode; the following year Nakamura demonstrated 1 candela InGaN based LED and at the same time Nichia announced its commercial blue LED. As LED's were fabricated, stage was set for arrival of lasers. In Jan 1996 Nakamura reported first pulsed blue InGaN laser at room temperature and at the end of the same year he announced first continuous wave blue GaN based injection laser at room temperature. During 1996 – 1997, quite a few groups reported InGaN-based LDs under room-temperature (RT) pulsed or continuous-wave (CW) operation, a summary of those work is shown in table below:

| Reference | Month, year | Group | Structure | | RT characteristics | Substrate |
|---|---|---|---|---|---|---|
| | | | Active layer | Type | | |
| 8 | 1, 1996 | Nichia | InGaN MQW | Stripe | Pulse | *C*-face sapphire |
| 9 | 2, 1996 | Nichia | InGaN MQW | Stripe | Pulse | *A*-face sapphire |
| 10 | 4, 1996 | Nichia | InGaN MQW | Stripe | Pulse | (111) spinel |
| 11 | 6, 1996 | Nichia | InGaN MQW | Stripe | Pulse | (111) spinel |
| 12 | 6, 1996 | Meijo | InGaN SQW | Stripe | Pulse | *C*-face sapphire |
| 13 | 9, 1996 | Nichia | InGaN MQW | Ridge | Pulse | *A*-face sapphire |
| 14 | 10, 1996 | Toshiba | InGaN MQW | Stripe | Pulse | *C*-face sapphire |
| 15 | 11, 1996 | Nichia | InGaN MQW | Ridge | CW (233 K) | *C*-face sapphire |
| 16 | 12, 1996 | Nichia | InGaN MQW | Ridge | CW (1 s) | *C*-face sapphire |
| 17 | 2, 1997 | Nichia | InGaN MQW | Ridge | Pulse | *C*-face sapphire |
| 18 | 2, 1997 | Nichia | InGaN MQW | Ridge | CW (40 min) | *C*-face sapphire |
| 19 | 3, 1997 | Nichia | InGaN MQW | Ridge | CW (27 h) | *C*-face sapphire |
| 20 | 3, 1997 | Nichia | InGaN MQW | Ridge | CW (35 h) | *C*-face sapphire |
| 21 | 5, 1997 | Nichia | InGaN MQW | Ridge | CW | *C*-face sapphire |
| 22 | 6, 1997 | Cree | InGaN MQW | Ridge | Pulse | 6H-SiC |
| 23 | 7, 1997 | Nichia | InGaN MQW | Ridge | CW (300 h) | *C*-face sapphire |

**Table 1 Early development of III-V Nitride based Laser Diodes**

After that there have been many break troughs in fabrication process as well as devices as listed below:

- In 1999 Nichia announced commercial violet laser diodes.
- In 2002 first planar hydride vapor phase epitaxy (HVPE) GaN was fabricated on *a*- plane
- In 2005 first planar hydride vapor phase epitaxy (HVPE) GaN was fabricated on *m*-plane GaN
- In 2005 Non polar laser diode on free-standing m-plane GaN substrates was demonstrated and high power *a* plane LED was demonstrated for first time.
- In 2006, Nonpolar /semipolar mechanism was developed followed by High power *m*- plane and high power semipolar LED.
- In March 2007, first demonstration of non polar m plane laser diode is made.

So overall there has been tremendous development in this dynamic field in last few years and UCSB group has been amongst most dominant group in bringing up innovation and stimulation to this field.

Such big research and industrial effort on GaN based LD is motivated by the superior properties of this material system which have indeed enabled the revolution in solid-state lighting and high-power/high-frequency electronics as well.

## 1.2 A (very) short summary of Nitride system

Compared other materials system, nitrides compounds have remarkable properties especially for lighting application because they offer a wide range of direct bandgaps from 0.7eV (InN) through 3.4eV (GaN) to 6.0eV (AlN) so they enable deep ultraviolet ($\lambda <\sim$ 300nm or photon energy $>\sim$ 4eV based on high Al content $Al_xGa_{1-x}N$ quantum wells [QWs]), ultraviolet ($\lambda < \sim$400 nm or photon energy > ~3.1 eV ), blue ($\lambda \approx$ 455nm or photon energy = 2.7 eV based on $In_yGa_{1-y}N$ QWs), and green ($\lambda \approx$ 525 nm or photon energy = 2.4 eV) emitters based on $In_xGa_{1-x}N$ QWs, and longer wavelength light-emitting diodes (LEDs) and violet and blue laser diodes (LDs) as shown in Fig. 4

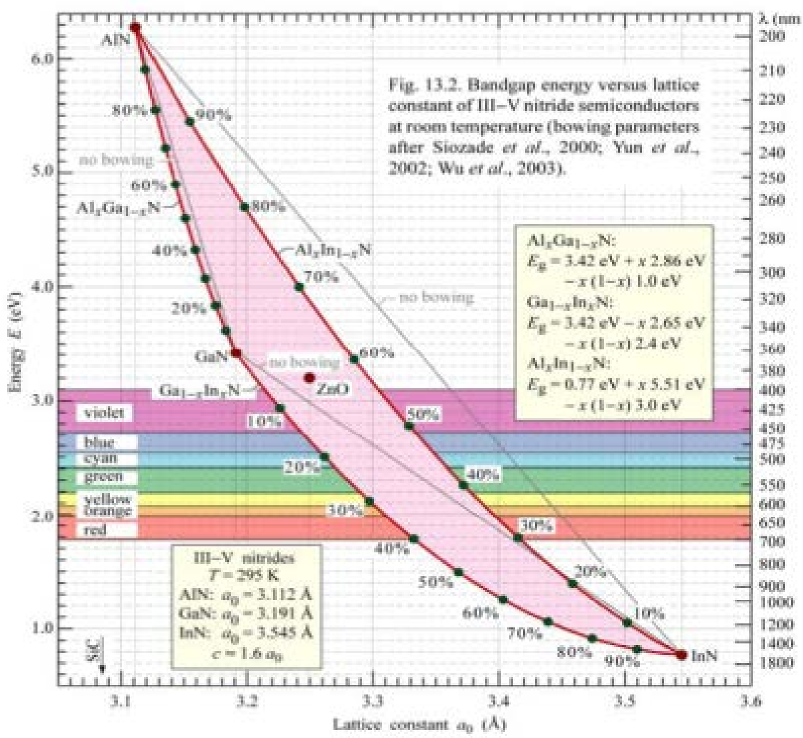


**Figure 3 The Nitride system [From 4]**

In this work all the samples have been grown on bulk m-plane GaN substrates. This is one of the most used non-polar plane and it is meant to improve the performace of the GaN devices because it does not suffer of the polarization effects typical of c-plane. Moreover, the LDs fabricated were all parallel to such c-axis in order to have with higher gain compared to the perpendicular direction

This c-plane is represented in Fig 2b and it is essentially the growth direction of the wurtzite structure typical of GaN and represented in Fig. 2a along the (0001) direction. It is currently the most used for blue LED and it is a polar plane.

Though commonly used for blue led and lasers, the c-plane has drawbacks, such as inducing electric fields that conspire to keep electrons and holes apart. The m-plane cuts across the crystal’s side: it doesn’t suffer from induced fields typical of the c-plane, but the substrates are more costly than c-plane versions. Semipolar substrates are generally cut at some angle to the crystal axis: they do not produce strong fields and they seem to yield better lasers and LEDs than the m-plane substrates do but are mostly in R&D phase and currently they are very expensive.

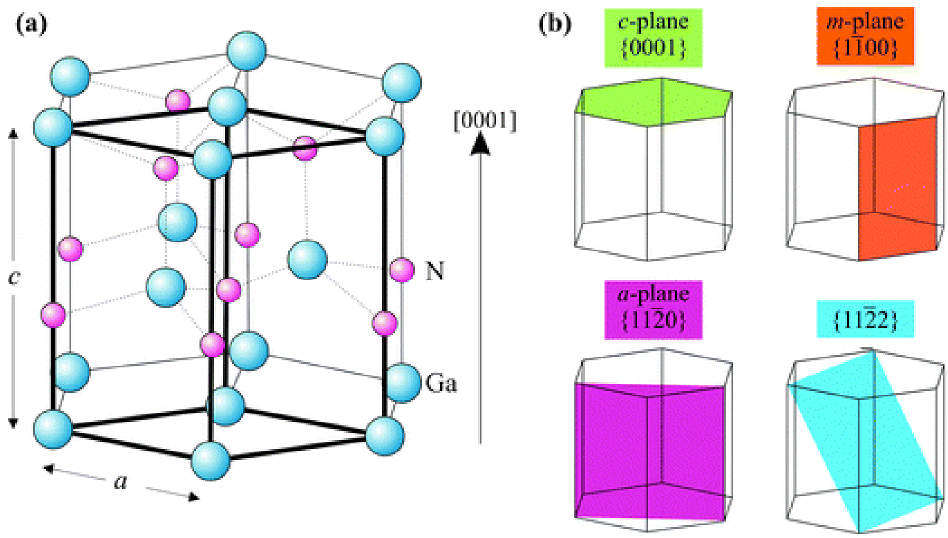


**Figure 4 Most commonly used GaN crystal planes**

Because the wurtzite structure is polar, GaN-based heterostructures have large internal electric fields due to discontinuities in spontaneous and piezoelectric polarization. For optoelectronic devices, such as light-emitting diodes and laser diodes, the internal electric field is generally deleterious as it causes a spatial separation of electron and hole wave functions in the quantum wells, which, in turn, likely decreases efficiency. Growth of GaN-based heterostructures in alternative orientations, which have reduced (semipolar orientations) or no polarization (nonpolar) in the growth direction, has been a major area of research in recent years, especially at UCSB.

### 1.2.1 Key features of c-plane

As anticipated above, the –c-axis is the direction along which it occurs parallel the spontaneous polarization caused by the hexagonal wurtzite structure which noncentrosymmetric (that is it lacks of absence of inversion symmetry) and it has space group P63mc and point group 6mm. Bernardini et al. computed the spontaneous and piezoelectric polarization (caused by the strain or tensile stress) for GaN, AlN, InN and derivates showing that their polarization is a bulk property and can be determined quantum mechanically with knowledge of the phase of the valence electron wave functions. InGaN QW is compressively strained because of the large lattice mismatch between GaN and InN ($\Delta a/a = 11\%$) and that induce piezoelectric polarization (PPZ) charges with an opposite sign to PSP to appear at the respective interfaces. The resultant polarization is generally dominated by PPZ which induces the internal polarization field (Fpol) to point from the top interface to the bottom interface and whose strength is as high as $1.74 MVcm^{-1}$ for blue $In_{0.15}Ga_{0.85}N$ LEDs.These huge internal polarization-related electric fields cause band bending profile explained in terms of Quantum Confinement Stack Effect (QCSE) or quantum confined Franz Keldysh effect (QCFK).

As a result, the following phenomena occur:

(1) a decrease in oscillator strength of electron–hole

(2) red-shift of the QW emission energy

(3) blue-shift of the emission energy with an increase in excitation density due to the reduction in the effective field strength by the Coulomb screening.

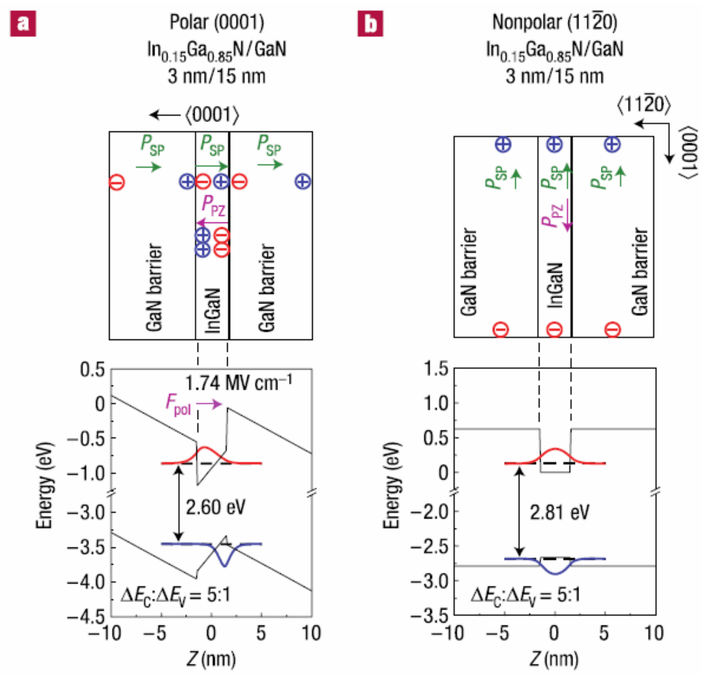


**Figure 5 QCSE in polar and non-polar planes [From 7]**

In particular spatial separation of electron and hole wave functions is detrimental for LEDs and LDs because it reduces the likelihood of a radiative recombination event[8], which yields the desired photon thus increasing the likelihood of the injected electrons or holes to nonradiatively recombine and squandering this energy as heat so it increases the so-called “efficiency droop”[9].

## *References*


[1] L.A. Coldren, S.W. Corzine, M. Marshanovitz, *Diode Lasers and Photonic Integrated Circuits*, pag. 24-39, 2nd Ed., Wiley, New York, (2012).

[2] H. Kroemer, *Quantum Mechanics For Engineering: Materials Science and Applied Physics*, Prentice Hall, (1994)

[3] S. Nakamura, S. J. Pearton, G. Fasol, *The Blue Laser Diode: The Complete Story*, Springer-Verlag, (2000)

[4] E.F. Schubert, *Light-Emitting Diodes*, Cambridge University Press, (2006)

[5] UCSB, *Materials 227 Course notes(* 2011)

[6] UCSB, *ECE 215C Course notes* (2011)

[7] J. S. Speck and S. F. Chichibu, MRS Bulletin, 34, 304, (2009)

[8] J.J. Wierer, J.Y. Tsao, and D.S. Sizov, Laser & Photon. Rev., 7, 963 (2013)

[9] D.F Feezell, MC Schmidt, SP DenBaars, S Nakamura, MRS bulletin 34, 318-323, (2009)

# Chapter 2

# Nitride Photo-Electro-Chemical (PEC) Etch

III-Nitrides compounds (In-Ga-Al/N) are chemically more stable than other III-V semiconductors. Their extreme lack of chemical reactivity make this material system resistant to traditional wet etching and chemical etching technique[1]. Unfortunately InAlGaN compounds are not easily wet-etched by any known chemical etchants: due to its very high chemical bond stability (8.92 eV/atom), GaN has proved resistant to all the acids and bases, with some mild etch of the N-face in hot KOH as the following table shows.

Table 1. Compilation of etching results in acid and base solutions, performed at room temperature (25°C) unless otherwise noted

| | GaN | InN | AlN | InAlN | InGaN |
|---|---|---|---|---|---|
| Citric acid (75°C) | 0 | 0 | 0 | 0 | 0 |
| Succinic acid (75°C) | 0 | 0 | 0 | 0 | 0 |
| Oxalic acid (75°C) | 0 | Lifts off | Lifts off | Lifts off | Lifts off |
| Nitric acid (75°C) | 0 | Lifts off | 0 | Lifts off | Lifts off |
| Phosphoric acid (75°C) | 0 | 0 | Oxide removed | Oxide removed | 0 |
| Hydrochloric acid (75°C) | 0 | 0 | 0 | 0 | 0 |
| Hydrofluoric acid | 0 | Lifts off | 0 | 0 | Lifts off |
| Hydriodic acid | 0 | 0 | 0 | 0 | 0 |
| Sulfuric acid (75°C) | 0 | Lifts off | 0 | 0 | 0 |
| Hydrogen peroxide | 0 | 0 | 0 | 0 | 0 |
| Potassium iodide | 0 | 0 | 0 | 0 | 0 |
| 2% Bromine-methanol | 0 | 0 | 0 | 0 | 0 |
| *n*-Methyl-2-pyrrolidone | 0 | 0 | 0 | 0 | 0 |
| Sodium hydroxide | 0 | Lifts off | Lifts off | Lifts off | Lifts off |
| Potassium hydroxide | 0 | Lifts off | 22,650 Å $min^{-1}$ | 0 | 0 |
| AZ400K Photoresist developer (75°C) | 0 | Lifts off | ~60–10,000 Å $min^{-1}$ | Composition dependent | 0 |
| Hydriodic acid/hydrogen peroxide | 0 | 0 | 0 | 0 | 0 |
| Hydrochloric acid/hydrogen peroxide | 0 | 0 | 0 | 0 | 0 |
| Potassium triphosphate (75°C) | 0 | 0 | 0 | 0 | 0 |
| Nitric acid/potassium triphosphate (75°C) | 0 | Lifts off | 0 | 0 | 0 |
| Hydrochloric acid/potassium triphosphate (75°C) | 0 | 0 | 0 | 0 | 0 |
| Boric acid (75°C) | 0 | 0 | 0 | 0 | 0 |
| Nitric/boric acid (75°C) | 0 | Lifts off | 0 | 0 | Lifts off |
| Nitric/boric/hydrogen peroxide | 0 | Lifts off | 0 | 0 | Removes oxide |
| $HCl/H_2O_2/HNO_3$ | 0 | Lifts off | 0 | Lifts off | Lifts off |
| Potassium tetraborate (75°C) | 0 | Oxide removal | Oxide removal | Oxide removal | Oxide removal |
| Sodium tetraborate (75°C) | 0 | 0 | 0 | 0 | 0 |
| Sodium tetraborate/hydrogen peroxide | 0 | 0 | 0 | 0 | 0 |
| Potassium triphosphate (75°C) | 0 | 0 | 0 | 0 | 0 |
| Potassium triphosphate/hydrogen peroxide | 0 | 0 | 0 | 0 | 0 |

**Table 2 Etching results for Nitride wet etchants**

For this reason InAlGaN device etching has traditionally been done by dry etching technique, for example Reactive Ion Etching (RIE), Inductively Coupled Plasma etching (ICP), Electron Cyclotron Resonant Etching (ECR), Chemically Assisted Ion Beam Etching (CAIBE) and Magnetron-reactive Ion Etching (MIE).

Currently all these etching methods for nitrides rely on Cl2- or sometime SF6-based physical dry etching. Although they allow a reasonable fast etching rate (up to few hundreds nm/min) and near-vertical sidewalls profile, these techniques have all two main big disadvantages.

First, they damage the device surface (most notably the p-GaN) and sidewalls and this damage is as higher as a high power – needed to have a reasonable etching rate – is used; such damage causes optical loss in optoelectronic devices, current loss in electronic devices and increase the surface recombination velocity which badly affect the device performance[2].

Surface recombination is modelled using SRH statistics[2]:

$$R_{sr} = \frac{a_S}{V} \cdot \frac{NP - N_i^2}{N/_{v_h} + P/_{v_e}}$$

Where N, P, $N_i$, $a_s$, V, $v_h$, $v_e$ are the the electron, hole, intrinsic carrier concentration, surface are, volume, hole and electron surface velocity respectively. The last parameter is dependent on the material system as summarized below

| Surface recombination velocity vs (cm/s) | |
|---|---|
| **InGaAs/GaAs (QW)** | ≈ 1 – 2 *10^5 |
| **GaAs (Bulk)** | ≈ 4 – 6 *10^5 |
| **InP (Bulk)** | < 10^4 |
| **GaN (Bulk)** | ≈ 10^4 – 10^5 |

**Table 3 Surface recombination velocity for different material system**

[2] The expression can be approximated as $R_{sr} = \frac{a_S}{V} \cdot v_s \cdot N$ at high level injection, regime where LDs typically operate

The device dimensions are also important and smaller devices are indeed affected more than bigger devices because the exposed surface area is bigger as depicted in Fig. 6

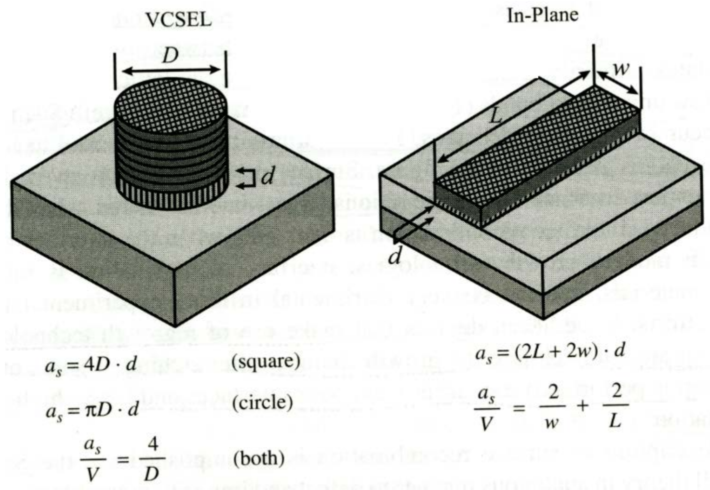


**Figure 6 [From 2] Comparison of surface area vs volume for different LD design**

Such dependence on device dimension is particularly important on edge emitting LDs which are meant to operate in single mode operation since in this case the maximum ridge width has to be < ~2um as from the equation:

$$w_{ridge} \cdot \sqrt{n_{ridge}^2 - n_{etched}^2(t)} < \frac{\lambda_0}{2}$$

with $\lambda_o$, $n_{ridge}$, $n_{etched}$, $w_{ridge}$ are the device emitted wavelength, the refractive index of the ridge, refractive index of the material surrounding the ridge and the ridge width as illustrated in Fig. 9

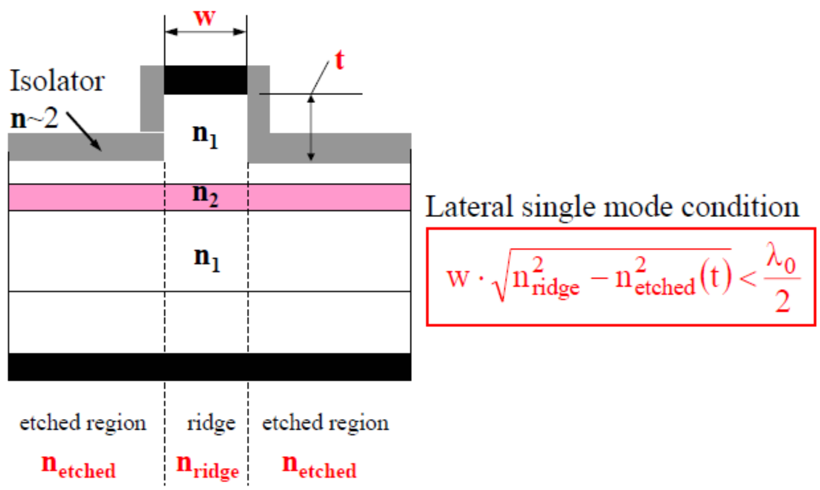


**Figure 7 Effective index scheme for ridge LD**

Another important drawback is that dry etching technique are in general not material selective and more importantly they do not allow to create undercut.

Indeed, wet etching techniques offer the possibility of lateral or isotropic etch compositional and crystallographic-selective etching[3] and they have been successfully applied to Si and other III-V semiconductors. Many studies have described the wet etching of InGaAsP compounds by mixtures of $H_2SO_4$:$H_2O_2$:$H_2O$, $C_6H_8O_7$:$H_2O_2$:$NH_4OH$, HCL:$H_2O$ and other acids/bases to fabricate complex optoelectronic devices such VCSEL, buried aperture oxide laser, constricted mesa laser and also electronic device such as InGaAs FinFETs[4-7].

Currently the only viable wet etching technique for Nitride is the Photo-Electro-Chemical Etch (PECE).

## 2.1 PEC Etching

PEC etching is a wet etching process and as such it offer all the advantages of the wet etching techniques.

This technique had been successfully applied already to Si and many III-V compounds[8]. It consists in illuminating with a supra-bandgap light source a sample immersed into a electrolyte which results in the generation of electron/hole pairs.

The semiconductor acts as anode, the metal deposited on the n-side acts as cathode and the conductive electrolytic medium which closes the circuit. The holes migrate to the surface which therefore becomes oxidized and finally etched by the electrolyte. In order to improve the photogenerated charges separation bias can be applied to the sample in such a way that it is reversed biased.

In Fig. 10 it is depicted a schematic of the common setup for PEC

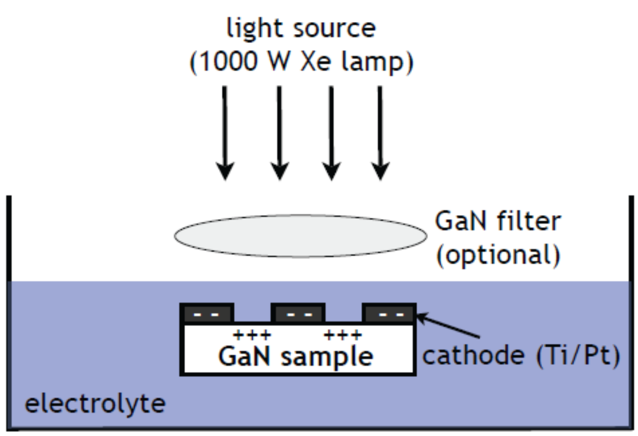


**Figure 8 Schematic of the PEC-Etch setup**

Many different types of solutions of either acid and basic pH and of different molarities have been reported ranging from HF to etch Si after photo-creating $SiO_2$ to $H_3PO_4$, $H_2SO_4$, HCL and KOH.

Along with the wet etching benefits, PEC etch offers other unique advantages:

- Bandgap selectivity
- Dopant selectivity
- Defect selectivity
- Crystallographic selectivity

In addition, it has been reported that PECE can recover the sample from the dry etching damage[9,10] as shown in Fig. 10

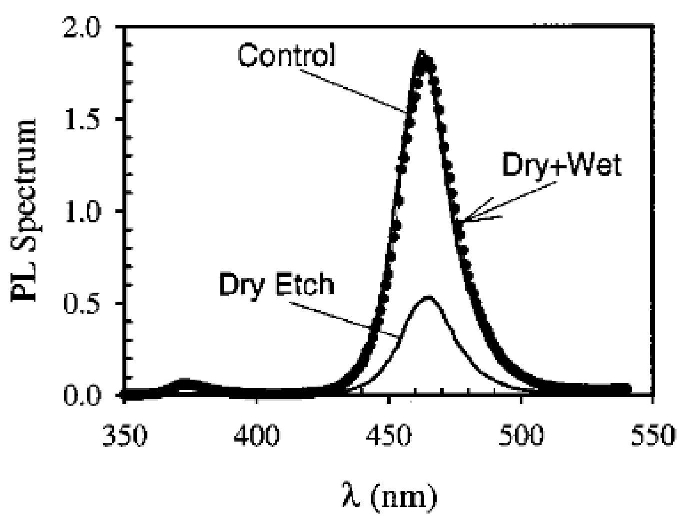


**Figure 9 Dry etching damage recovery after PECE wet etching [From 10]**

The ability of the PECE to recover the damage produced by the dry etching damage is important both for electronic device and optoelectronics devices, especially for laser diodes. Indeed dry etching causes a degradation of the LD performance, both by increasing the device threshold current and by lowering the device slope efficiency as shown below:

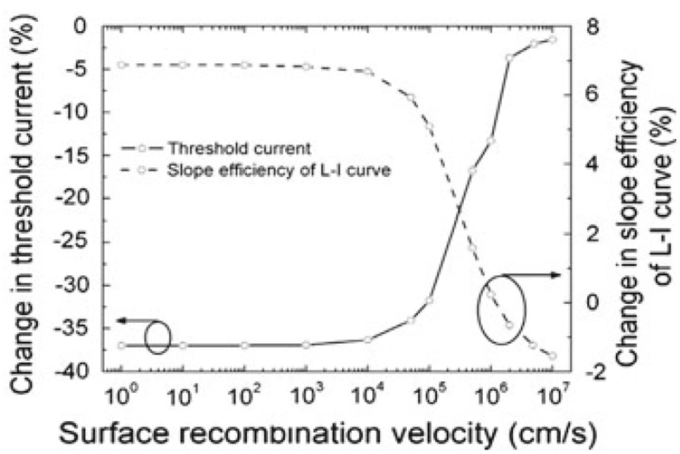


**Figure 10 Change in threshold current vs surface recombination [From 11]**

## 2.2 PEC applied to Nitride

Although the idea of anodic-etching GaN dates back to the early '60s[12], GaN photo-electrochemical etching has been successfully achieved only in the mid-90s'[13]. Several studies have reported the etching of n-type GaN producing whiskers and surface with different degrees of roughness depending essentially on the quality of template, light power intensity, bias applied and solution stirring[14-16]. Several electrolytes at different concentration have also been tested[17] ranging from

$H_2SO_4$:$H_2O_2$ to KOH, HF:$HNO_3$ and HF:$C_2H_5OH$ and KOH, with this last now established as the most commonly used electrolyte. In general, a low concentrated and a slowly stirred solution favor a smoother etched surface. A p-GaN/InGaN/n-GaN p-i-n structure has been used to etch p-type GaN, which has been notoriously more difficult to PEC-etch because of the unfavorable band-bending at the interface p-semiconductor /electrolyte. By this mean, complex electronic and optoelectronics devices like CAVET transistors and microdisk lasers, porous GaN structures, photonic crystals embedded in GaN LEDs and more recently VCSEL fabricated in m-plane have been obtained[18-20].

Sacrificial GaN-based layers wet etching have been proved to be even more challenging. To the best knowledge of the authors, no good control of the lateral profile and at the same time of the selectivity has been reported for any GaN-based materials wet etching. LEDs sidewalls roughening, etching of the active region and at the same time the n-side layer along the 10-10 crystal plane and of the p-side at an angle of 27° with respect to the 10-1-1 plane have been reported[21,22], while sacrificial layers have been employed to remove the substrate[23,24]. In general, in all these studies a relatively high bias (up to 20V) has been applied, and the etching is usually achieved in two different times, with the actual etching following the oxidation step (1um/h). Furthermore no control of the etch profile has been provided. Other groups[25,26] have focused their attention on AlInN/GaN structure, where the AlInN layer has been selectively oxidized and etched from GaN with different oxidation/etching rates and microbridges, planar microcavities and microdisk lasers have been reported. Metal mask have been used only as contact to bias the sample and their effect have only been studied to understand the enhancement of etching rate near their border and the trenching effects they had caused, this last phenomenon explained in terms of electron capture by the metal which therefore enhance the probability of the holes to oxidize the semiconductor and therefore its subsequent etch[27.]

## 2.3 Control of the PEC-etched active region

The first goals of this research have been:

- PEC-Etching the active region embedded into a complex p-i-n structure. Previous works at UCSB have successfully shown the PEC-Etching of the active region embedded into a n-i-n structure.

- Controlling the PEC-Etching, in particular it is important to stop the etching process at some desired point of the epitaxial structure.

To these goals, we have grown several samples by MOCVD on free standing (FS) m-plane GaN template provided by Mitsubishi Chemical Corporation (MCC) according to the following structure: a low temperature nucleation layer, 200nm-

800nm n-GaN, 50nm n-InGaN waveguide (~6% In), a series of InGaN/GaN MQWs, 20nm AlGaN EBL, 50nm p-InGaN (~6% In), a p-GaN with a small p++-GaN layer on top. N- and p- type doping levels are estimated to be in the order of $10^{19}$ and mid-$10^{17}$ respectively, the In composition of the MQW was ~15 – 18% based on PL measurements. By lithography we patterned stripes of different width and length which have been oriented either along the (0001) direction or along the 11-20 a-direction, being the first orientation typically used to fabricate optoelectronics devices (the material gain is maximized), while the second orientation was chosen to study the different etching rate of the c+ and c- face along with the fact that 11-20 is a natural cleaving plane for m-plane GaN. A thick $SiN_x$/SiO2 (~1.5um) deposited by Advanced PECVD followed the deposition of a thick metal stack Pd/Au (200/5000A) deposited by ebeam evaporation. We created mesa structures by Cl2-based RIE etching the stripes down through the p-GaN. The resulting structure was covered again with $SiN_x$ (~200nm) so that p-GaN surface if oxidized by the photogenerated holes overflowing from the quantum wells would not be exposed and therefore etched by the electrolyte solution[29]. On the backside of the samples we deposited 100/5000A Ti/Au layer for the n-contact. Finally the samples were then deeply etched again using the previously SiNx mask (self-aligned process) in order to expose the MQWs and part of the n-GaN layer. Before we proceeded with the actual PEC-etching step we have immersed the sample into a HCL solution under dark illumination for few minutes to remove the native oxide.

A short schematic of the flow process and the final structure of a sample before the PECE step is depicted in Fig. 13

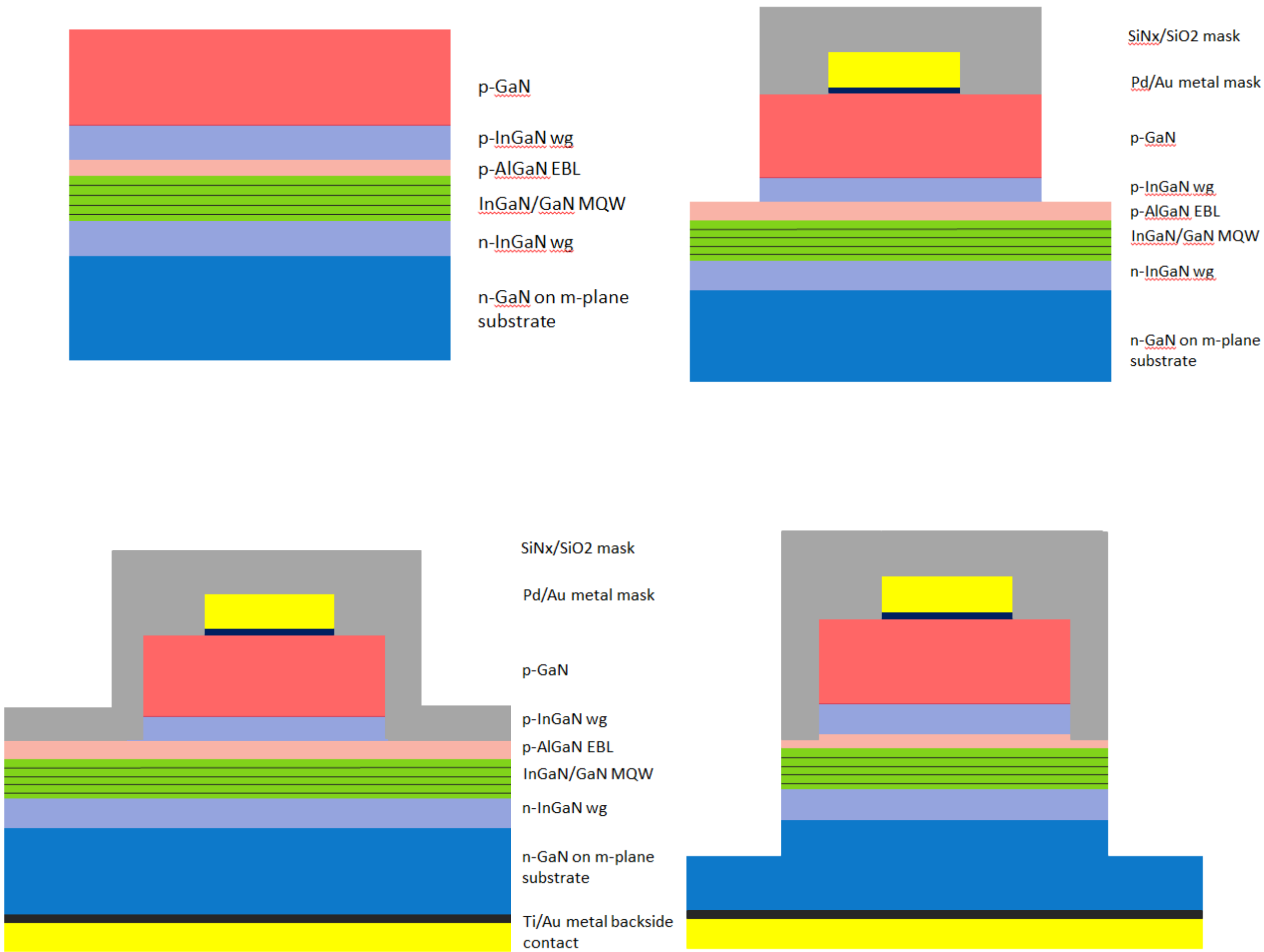


**Figure 11 Schematic of the flow process**

The PEC etching was performed by dipping the samples into a 1Mol KOH solution at room temperature, an external bias was applied only in the very first experiments. All the results presented in this thesis have been obtained with no bias applied.

As light source to generate the excitons into the active region both a fluorescence microscope (Olympus Eclipse LV150, emission range: 380-420nm, light output power: 13.6 mW/cm$^2$ as measured by a calibrated photodetector), a violet laser diode ($\lambda$ = 405nm) and a broadband white lamp (Oriel, 68806 Basic Arc Lamp), with a GaN filter were used as it is illustrated. A schematic of the setup most commonly used in these experiments and photos of the final setup are presented in Fig. 14

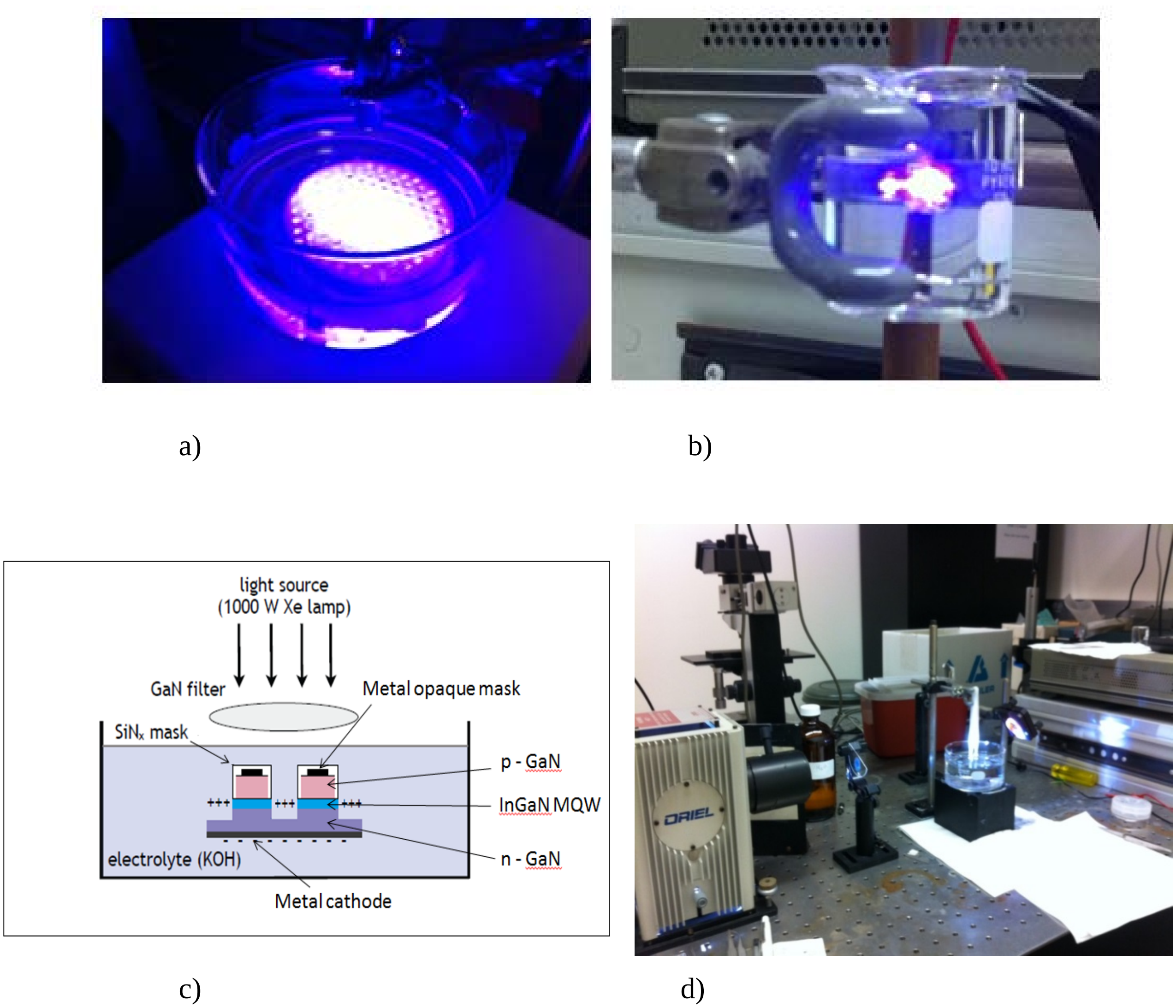


**Figure 12 Setup used for PECE experiments**

After etching, the samples were rinsed in DI water, N2-blow dried and characterized by optical microscope using a Nomarski filter for differential interference contrast (DIC) imaging (Olympus LG-PS2). A fluorescent microscope was used both to provide the light necessary to generate the electron-hole pairs needed for the PECE process to start and to monitor *in-situ* the proceeding of the active region etching by looking at the shrinking of the fluorescent region. The samples were etched until all the stripes did not lit up anymore as it can be seen in Fig 15b.

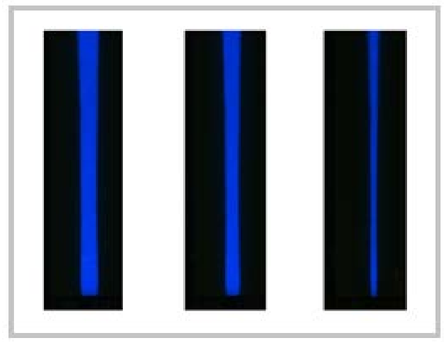

**a)**

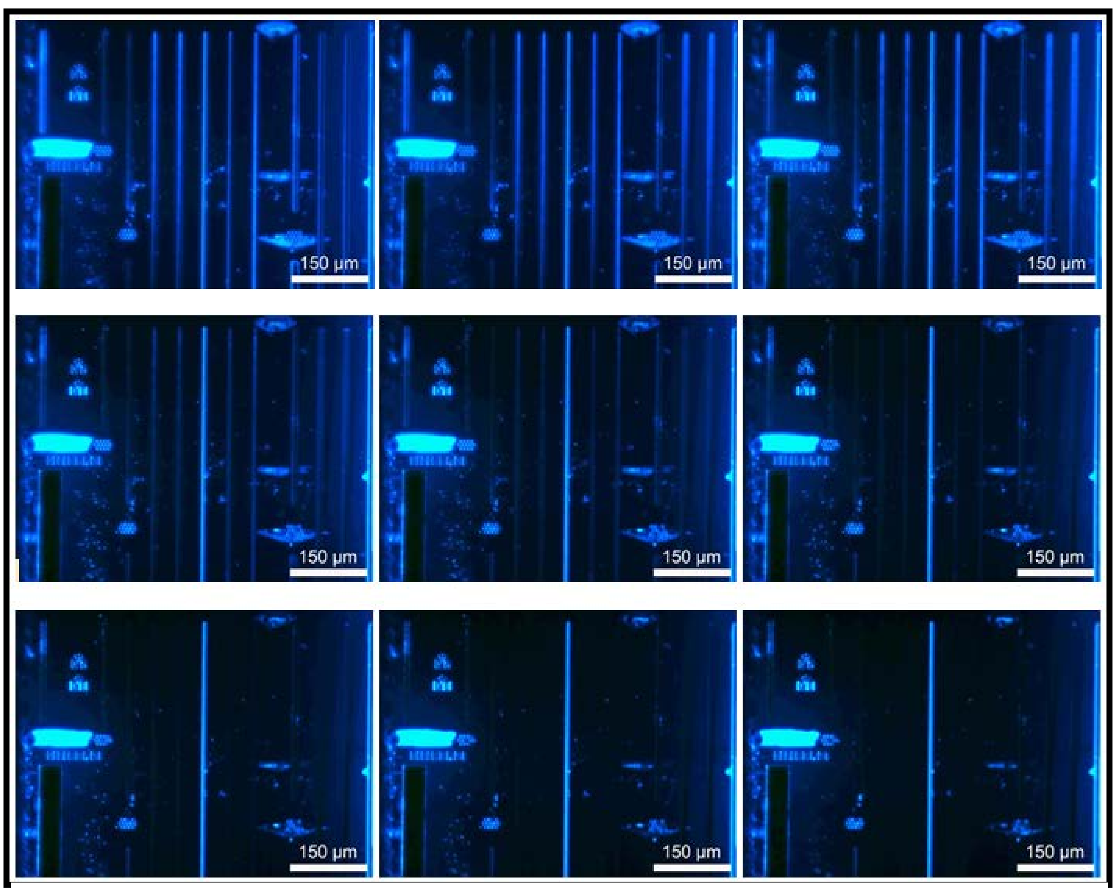


**Figure 13 a) Details of a PECE stripe, b) multiple stripes etched**

We proceeded in a similar way with the stripes that had on top the metal opaque mask meant to block the light and therefore the photogeneration of the electron/hole pairs needed to the PEC-etch process to start.

After removing the metal and SiN mask by HF and Au etchant respectively, we observed a fluorescence region area which corresponded to the area covered by the opaque metal mask during the PEC etching, as observed in Fig.

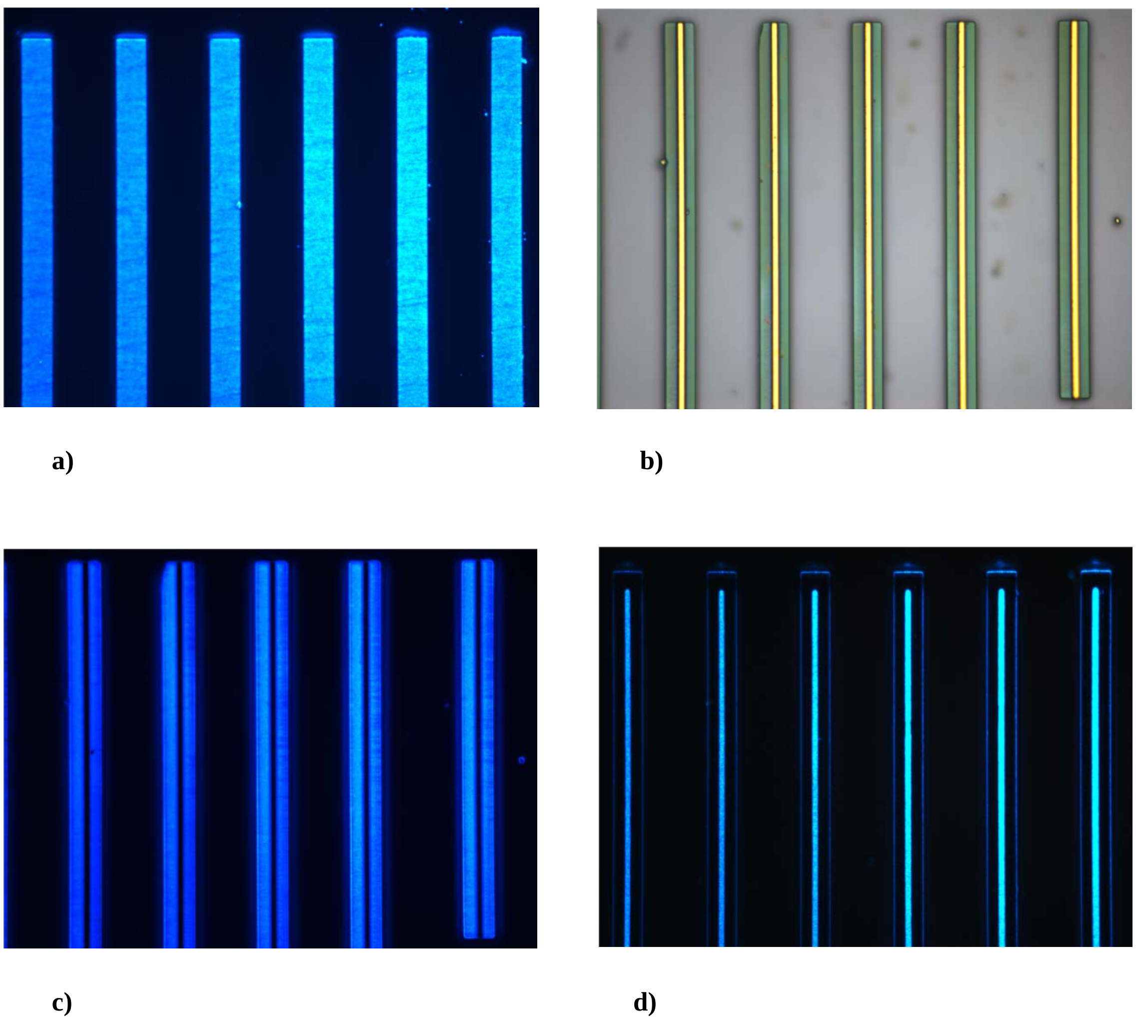


**Figure 14 Fluorescent stripes a) before and after d) the PEC Etching**

Finally we cleaved and analyzed the stripes with scanning electron microscopy (FEI Sirion and JEOL 7600F). The SEM images have revealed that the etching had indeed occurred at the MQWs and then it stopped at the edge of region where the light absorption was blocked by the opaque mask.

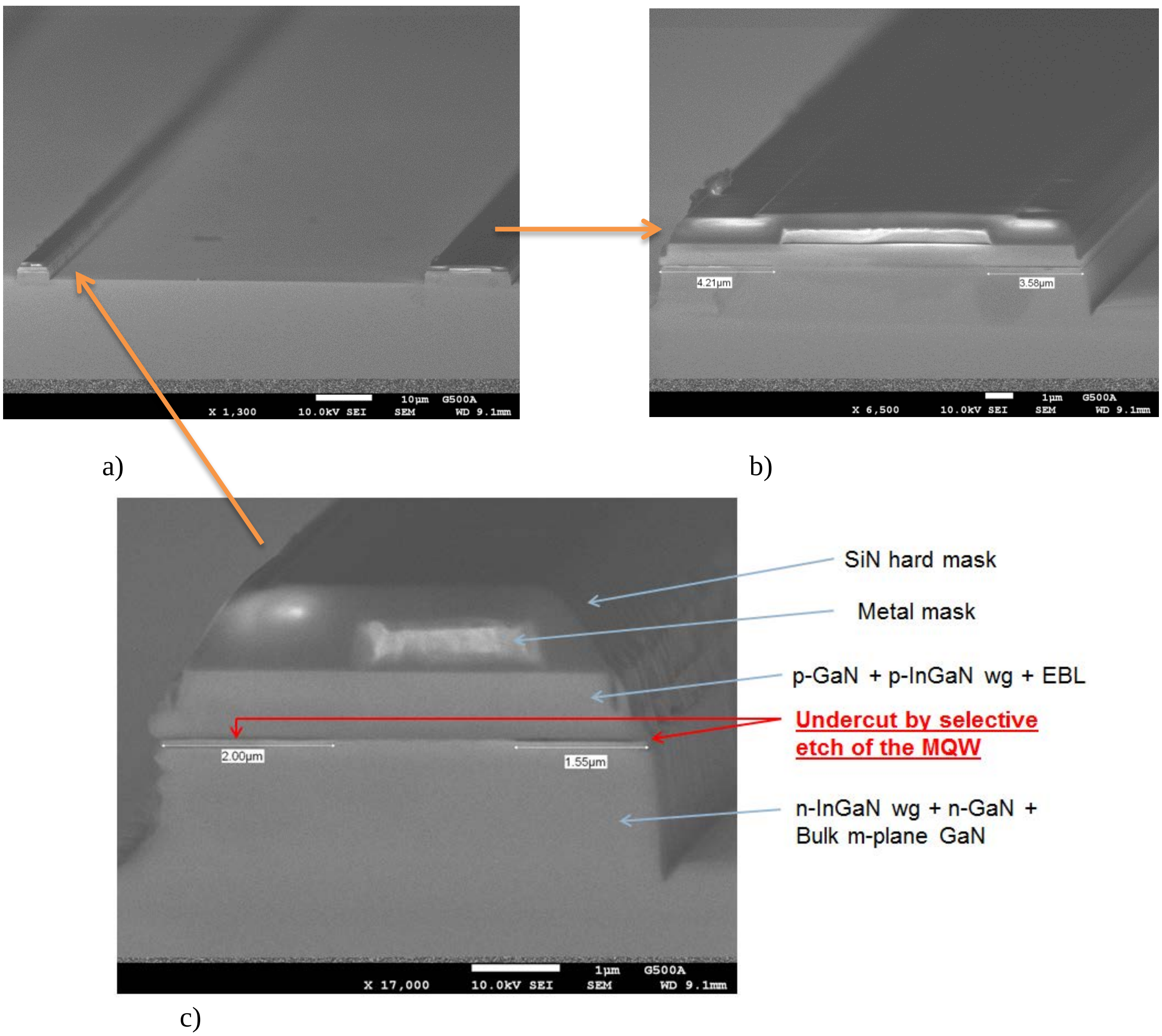


**Figure 15 SEM images of two stripe located close on the samples and PEC- etched at the same time, b) and c) details on the front face of the two stripes has evidenced that the PEC-Etch stopped very close to the edge of the opaque metal mask**

We noticed that both the Ga (c+) face and the N (c-) face were PEC-etched. The N-face is known to be more chemical reactive than the Ga-face and on the c-plane the N-face etches with typical crystallographic pyramidal-shape profile while the Ga face is essentially not etched at all. On other hand on m-plane the intrinsic polarization field pushes the hole towards the Ga face which as results etches even faster than the N-face. We measured the different etching rate of the Ga and N face and for different set of samples we calculated that Ga-face etched was 2.5x – 4x faster then the N-face. We recorderd various etching rate for different samples, although the epitaxial structure was similar, with etching rate ranging from few tens nm/min up to ~1.2um/min. We believe that such big difference in etching rate might be attributed to small fluctuations in the quality of the epitaxial structure. This cause may also be responsible for the fact that few stripes were not etched at all although they were close located to other stripes that etched correctly as Fig. 15 shows.

Indeed PEC-etching is a technique very sensible to the material quality and uniformity. Defects and threading dislocations can cause a leakage current[29] and act as effective recombination centers favoring the excitons recombination which in turn impede the etching. This is shown in Fig. 18 where local nano-regions (∼100nm) have not been etched although the electrolyte could percolate through the small gap produced by the etched active region (~50nm).

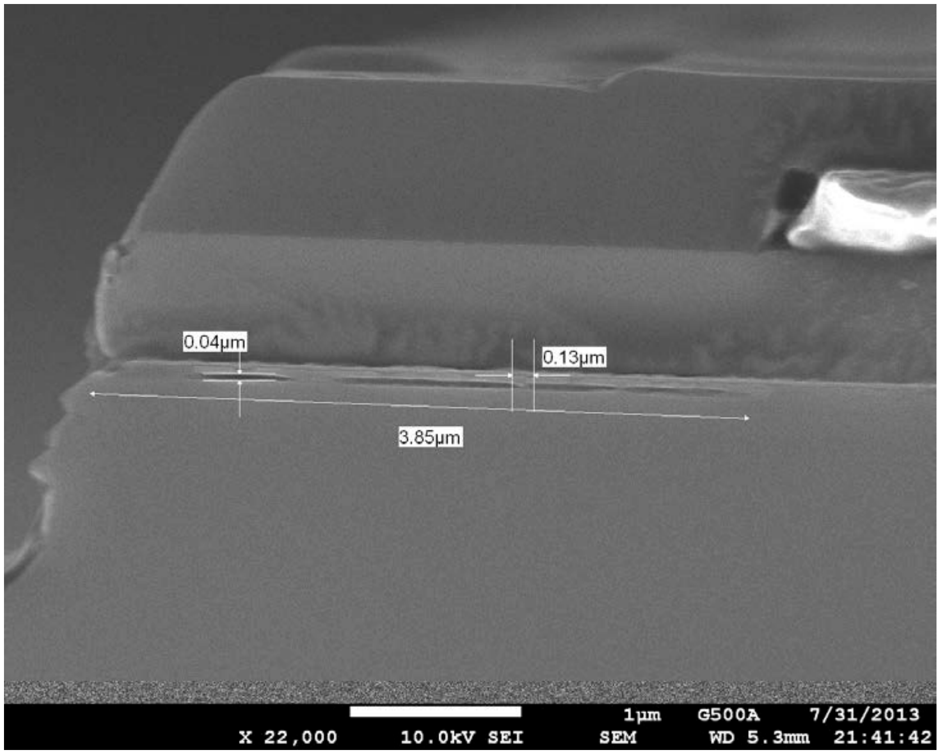


**Figure 16 Details of a different stripe showing again the stopping of the PEC-etch at the edge of the opaque metal mask, the nano-regions which did not etch and the tapered shape profile of the undercut obtained by the PEC-Etch**

PEC etching relies indeed on three main competing mechanisms: (i) generation and separation of the excitons, (ii) surface oxidation and (iii) etching of the oxidized semiconductor surface. For the PEC etching to work properly the excitons generation and separation rate and the hole diffusion time to surface have to occur on same time scale of the etching rate, meaning that the oxide formed has to be removed very quickly. Alternatively the photogenerated holes can either recombine immediately with the electrons or they can escape from the QWs to the p-GaN and cause the etching there. Further studies are undergoing to analyze how using a better material quality can improve the PEC-E process. A careful analysis of the SEM images has also revealed that in several stripes the etching did not stop exactly at the edge of the dark region produced by the opaque metal mask. In other material systems such PEC-etch resolution has been related[30] to the hole diffusion length $L_h = \sqrt{D_h \tau_h}$ . As a consequence, the un-illuminated semiconductor region which is within $L_h$ can still be oxidized by the holes and therefore etched. However, this argument does not explain by itself the deep undercut that we observed (in some cases on the order of ~350nm), even assuming the fastest etch rate we measured for some set of samples. Indeed we believe that the major role in determining the PECE resolution is due to scattered light, possibly from the rough backside surface. Eventually the insertion of an InGaN absorbing layer (for example made an InGaN layer or an InGaN/InGaN superlattice) between the active region and the backside contact may help improving the PECE resolution. We noted also a tapered shape profile at the end of all the etched structure, as it has been also observed in the PEC-Etch of other material system[31-34] as shown in Fig. 18 . This has been attributed to the local enhancement of the electric field at curved interface[35] produced by holes local accumulation in the space charge region.

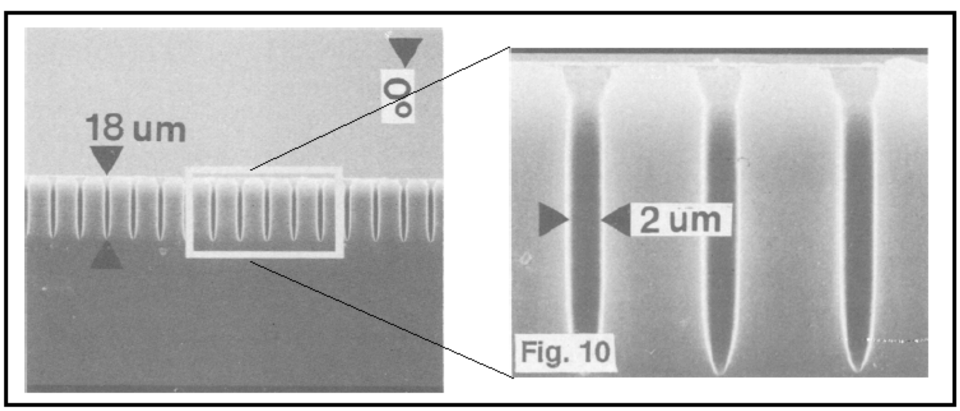


**Figure 17 Tapered PEC-Etched profile in GaP**

## References

[1] S.J. Pearton, F. Ren, R.J. Shul, C-S. Wu, MRS Proceedings, 421, (1996)

[2] L.A. Coldren, S.W. Corzine, M. Marshanovitz, Diode Lasers and Photonic Integrated Circuits, pag. 24-39, 2nd Ed., Wiley, New York, 2012.

[3] K. Hjort, *J. Micromech. Microeng.* **6**, 370, (2005)

[4] M. M. Dummer, J. R. Raring, J. Klamkin, A. Tauke-Pedretti, and L. A. Coldren, *Opt Express*., **16**(25), 20388-94, (2008)

[5] D. Pasquariello, E. Bjorlin, D. Lasaosa, Y.-J. Chiu, J. Piprek, and J. Bowers, *J. Lightwave Technol.* **24**, 1470–1477, (2006).

[6] Y.-J. Chiu, T.-H. Wu, W.-C. Cheng, F. Lin, and J. Bowers, *IEEE Photon. Technol. Lett.* **17**, 2065–2067, (2005).

[7] T. Kitano, S. Izumi, H. Minami, T. Ishikawa, K. Sato, T. Sonoda, and M. Otsubo, *Vac. Sci. Technol. B* **15**, 167 (1997).

[8] P. A. Kohl and F. W. Ostermayer, Jr., *Annu. Rev. Mater. Sci.* **19**, 379-99, (1989)

[9] M. Mosca, A. Castiglia, H.-J. Bühlmann, J. Dorsaz, E. Feltin, J.-F. Carlin and N. Grandjean, The European Physical Journal Applied Physics, Vol. **43**, 1, 51-53, (2008)

[10] M. Boroditsky , I. Gontijo , M. Jackson , R. Vrijen , E. Yablonovitch , T. Krauss, C. Cheng , A. Scherer , R. Bhat and M. Krames, J. Appl. Phys. **87** , 3497 (2000)

[11] Md. Mahbub Satter, P. D. Yoder, Optical and Quantum Electronics, **42**, 11-13, 747-754, (2011)

[12] J. Pankove, Electrolytic Etching of GaN, J. Electrochem. Soc. **119**,1118, (1972)

[13] M.S. Minsky, M. White, E.L. Hu, Room-temperature photoenhanced wet etching of GaN, Appl. Phys. Lett. **68**, 1531, (1996)

[14] C. Youtsey, I. Adesida, G. Bulman, Appl. Phys. Lett. **73**, 797, (1998)

[15] C. Youtsey, I. Adesida, L.T. Romano, G. Bulman, Appl. Phys. Lett. **72**, 560, (1998)

[16] P. Visconti, M. A. Reshchikov, K. M. Jones, D. F. Wang, R. Cingolani, H. Morkoç̌, R. J. Molnar, and D. J. Smith, J. Vac. Sci. Technol. B **19**, 1328 (2001)

[17] K. Al-Heuseena, M.R. Hashima, N.K. Alib, Applied Surface Science Volume **257**, 14, 6197–6201, (2004)

[18] Y. Gao, I. Ben-Yaacov, U. K. Mishra, and E. L. Hu, Journal of Applied Physics, **96**, 11, (2004)

[19] A. C. Tamboli, E. D. Haberer, R. Sharma, K. H. Lee, S. Nakamura and E. L. Hu, Nature Photonics **1**, 61 – 64, (2007)

[20] C.O. Holder, J. S. Speck, S. P. DenBaars, S. Nakamura, and D. Feezell, Demonstration of Nonpolar GaN-Based Vertical-Cavity Surface-Emitting Lasers, Appl. Phys. Express **5**, 092104, (2012)

[21] Chia-Feng Lin, Zhong-Jie Yang, Jing-Hui Zheng, and Jing-Jie Dai, IEEE PHOTONICS TECHNOLOGY LETTERS, **17**, 10, (2005)

[22] C. Yang, C. Lin, J. Chiang, H. Liu, C. Lin, F. Fan, C. Chang, Journal of Electronic Materials, **38**, 145, (2009)

[23] D. Kim, H. Chang, H. Cha, H. Jeon, and S. Jeon, Appl. Phys. Lett. **102**, 152112, (2013)

[24] A. R. Stonas, T. Margalith, S. P. DenBaars, L. A. Coldren, and E. L. Hu, Appl. Phys. Lett., **78**, 1945 (2001)

[25]F. Rizzia, K. Bejtkaa, P.R. Edwards, R.W. Martin, I.M. Watson, Journal of Crystal Growth **300**, 254–258, (2007)

[26] D. Simeonov, E. Feltin, H.-J. Bühlmann, T. Zhu, A. Castiglia, M. Mosca, J.-F. Carlin, R. Butté, and N. Grandjean, Applied Physics Letters, **90**, 6, (2007)

[27] J. Skriniarova´a, A. van der Hart, H.P. Bochem, A. Fox, P. Kordos, Materials Science and Engineering B, **91**, 298-302, (2002)

[28] A. C. Tamboli, M.C. Schmidt, S. Rajan, J.S. Speck, U. K. Mishra, S.P. DenBaars, and E. L. Hu, Journal of The Electrochemical Society, **156** 1 H47-H51 (2009)

[29] D. S. Li, H. Chen, H. B. Yu, H. Q. Jia, Q. Huang, and J. M. Zhou, J. Appl. Phys. **96**, 1111 (2004)

[30] F. W. Ostermayer, P. A. Kohl, and R. M. Lum , J. Appl. Phys. **58**, 4390 (1985)

[31] E. Mannheim, R.C. Alkire, . L. Sani, J. Electrochem. Soc., **141**, (1994)

[32] V. Lehmann and H. Föll, J. Electrochem. Soc., **137**, 2, (1990).

[33] X. G. Zhang, Mechanism of Pore Formation on n-Type Silicon, J. Electrochem. Soc. , **138**, 12, (1991)

[34] B. H. Erné, D. Vanmaekelbergh and J. J. Kelly, J. Electrochem. Soc., **143**, 1, 305-314, (1996)

[35] M. Sze and G. Gibbons, Solid-State Electron., **9**, 831 (1966).

# Chapter 3

## Nitride Current Aperture Blue Laser Diode

Since the invention of the blue laser diode (LD) in early ‘90s by Nakamura[1], significant progress has been made in developing high efficient and high power LDs. Already employed successfully in a variety of applications ranging from biomedical devices to scientific instruments and consumer electronics, blue LDs look promising also for Solid State Lighting[2] and high frequency light-based communication[3] (Li-Fi).

Along with the carefully engineering of the device epitaxial structure, both a tight carriers-current-photons confinement into the active region and the reduction of the series resistance are necessary to improve the LDs wpe. To this purpose, several designs of edge-emitting LDs have been proposed8, each having a different degree of complexity and fabrication cost in terms of growth and processing steps. Between the cheapest and simplest gain guided and the very expensive and complex buried-ridge-stripe laser, the etch ridge design represents an acceptable compromise in terms of performance, device lifetime and cost. Although it offers a better reliability, the shallow etch ridge design provides also leaky paths for carriers and current, differently from the deep etch ridge design in which the laser ridge is etched though the active region and therefore no leaky paths exist. In device performance terms this translates into a lower threshold current, higher optical output power and more generally into a higher wpe, as both simulations9 and experimental10 works have demonstrated.

Fig. 18 presents the most common LD ridge design

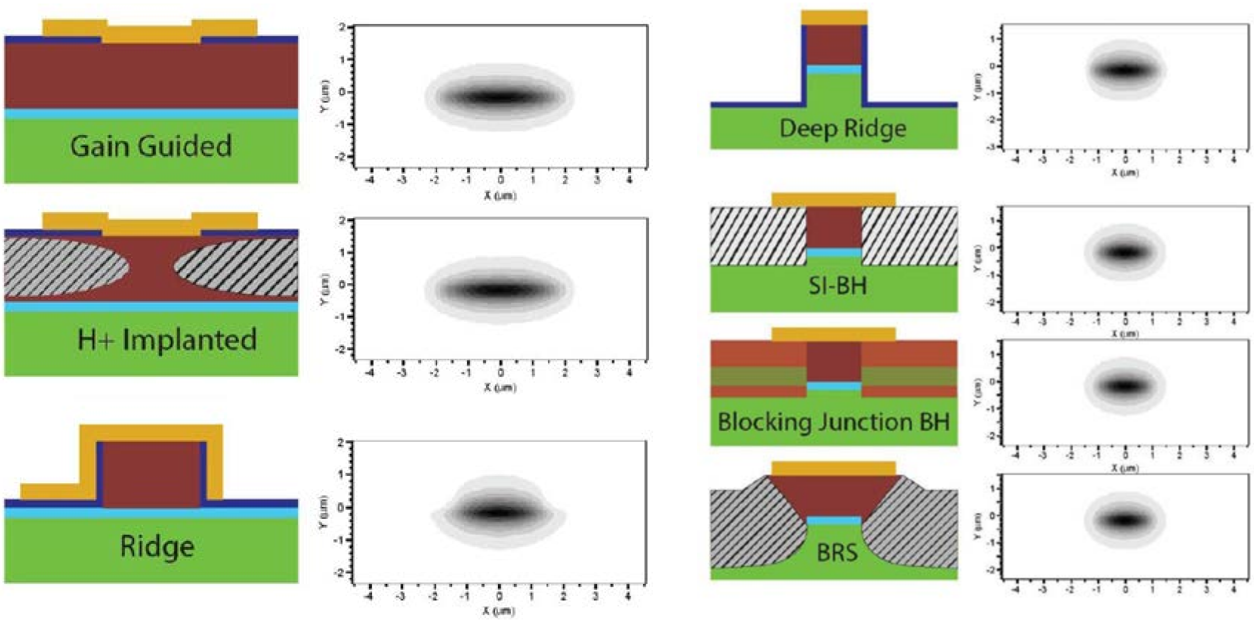


**Figure 18 Most common LD ridge design**

Decreasing series resistance is also very important to achieve highly efficient LDs. This is not dependent on ridge etch depth and it is especially relevant for devices which need to have small width dimension (<2.5um) for single transverse mode lasing. The total operating voltage of a LD can indeed be expressed as $V_{tot} = V_d + IR_s$, with the first term being the diode voltage and IRs the voltage drop on the rest of the device. A voltage inefficiency factor representing the voltage that needs to be applied in excess of the junction voltage can thus be defined as $(1-V_d)/V_{tot}$ and it may account for as much as ~40% of the total ineffiencies (1-wpe) in current high performance blues LDs.

Current aperturing has indeed been used to fabricate photonic devices in other III-V systems by exploiting selective composition and crystallographic wet etching[12-14] which is not possible to achieve in the nitride system using common wet etchants, or by selective oxidation and regrowth steps[15-16]. This last technique has also been used to fabricate GaN current aperture vertical electron transistors[17] (*CAVETs*).

The distinctive feature of the current aperture laser (CA-laser) design is represented by the reduced lateral dimension of the active region whose area is therefore smaller than the as-grown bottom n-doped and top p-doped regions. This is obtained through a selective and a controllable etch of the MQW active region by photo-electro-chemical etching (PECE) which follows the laser ridge deep etch step.

The CA-laser offers superior advantages with respect to the shallow etched ridge laser. Indeed comparing the two designs, the CA-laser (i) provides a higher current-carrier-photons confinement, (ii) eliminates any leakage paths because of the laser ridge deep etch, (iii) offers a reduction in series resistance because of the wider p-GaN region, while maintaining an equal area of active region and injection efficiency, (iv) offers superior performances for high speed applications. Simulation done using FIMMWAVE[18], a commercially available 2D waveguide mode solver, have shown that the confinement factor is similar for the two designs as shown in Fig. 19.

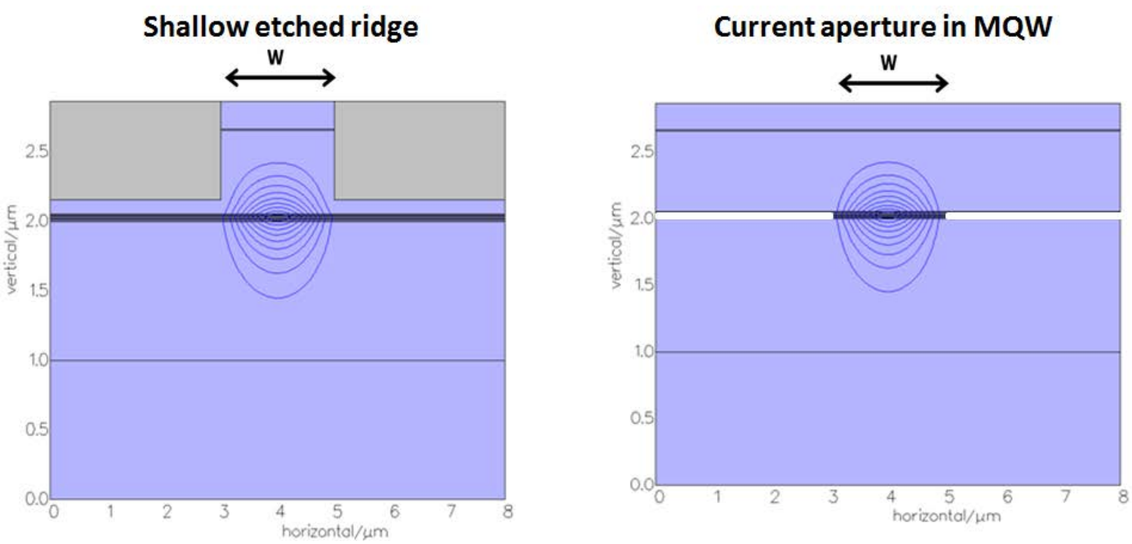


**Fig. 19 Simulation of the optical mode in the shallow etched (left) and current aperture deep etched laser structure. Courtesy Dr. Cohen**

### 3.1 Fabrication of Nitride-based Current Aperture laser

Hereafter, we report the fabrication of a nitride current-aperture laser (also denominated constricted mesa laser11), to the best knowledge of the authors a design realized for the first time in nitride-based optoelectronics.

We have grown LDs structures by atmospheric-pressure MOCVD on free standing (FS) m-plane GaN substrate provided by Mitsubishi Chemical Corporation (MCC). The epitaxial structure consisted of a low temperature nucleation layer, 800nm Si-doped n-GaN, 50nm Si-doped n-InGaN waveguide layer (~6% In), a series of InGaN/GaN MQWs (~4.5/11nm), 20nm Mg-doped p-AlGaN (15% Al) electron blocking layer (EBL), 50nm Mg-doped p-InGaN (~6% In, [Mg] ~mid-$10^{17}$), 800nm p-GaN with a small p++ Mg-doped GaN layer on top. The In composition of the MQW was estimated ~16 - 18% based on PL measurements.

CA-LD have been fabricated according to the following flow process. Opaque metal mask stripes of different width and length were defined by standard UV-lithography along the c+ direction and deposition of a thick metal layer (Pd/Au 300/5000A) by ebeam evaporation, followed by a blank deposition of a thick ~1.5um low-stress SiNx/SiOy layer by Advanced-PECVD. Both these insulators are transparent to UV-light radiation and the purpose of such stack is to alleviate the possible bending or breaking of the structure by reducing the layer total internal strain, having the $SiO_x$ ($SiN_y$) an internal (compressive) stress respectively.

The LD bars geometry was defined on top of the opaque metal mask by a CF4/CHF3-based ICP etch of the SiOx/SiNy layer. These insulator stripes were then used as hard mask for the subsequent Cl2-based RIE etch of the p-GaN. The resulting structure was covered again with $SiO_x/SiN_y$ (~100nm) in order to have the p-GaN surface not exposed to the electrolyte during the PECE. Indeed the p-GaN surface oxidized by the photogenerated holes overflowing from the quantum wells would be etched by the electrolyte solution[20].

On the back side of the samples a 100/5000A Ti/Au layer was deposited as a n-contact. The samples were then deeply etched again down to part of the n-GaN layer by a self-aligned process using the previously SiNx mask in order to expose the MQW for the subsequent PEC etch step. After dipping the samples into a HCL solution in a dark environment for few minutes to remove the native oxide, we proceeded with the actual PEC etch of the MQW. This was done by immersing the samples into a 1Mol KOH solution at room temperature without applying any external bias. A broadband white lamp (Oriel, 68806 Basic Arc Lamp) provided with a GaN filter was used as light source. The etching of the MQW layer stopped very close to shadowed region defined by the opaque metal mask whose role was indeed to stop the photogeneration of the electrons and holes pairs which are necessary for the PECE process to start. Although not used for PEC-etching, it is worth to mention that KOH treatment has been reported to be also beneficial to recover both optoelectronics and electronics device surface from the dry etch damages[21,22]. The insulator and metal opaque mask were then removed using HF and Au etchant respectively and we checked the result of the PECE by observing the shrinking of the fluorescence active region as shown in Fig. 2

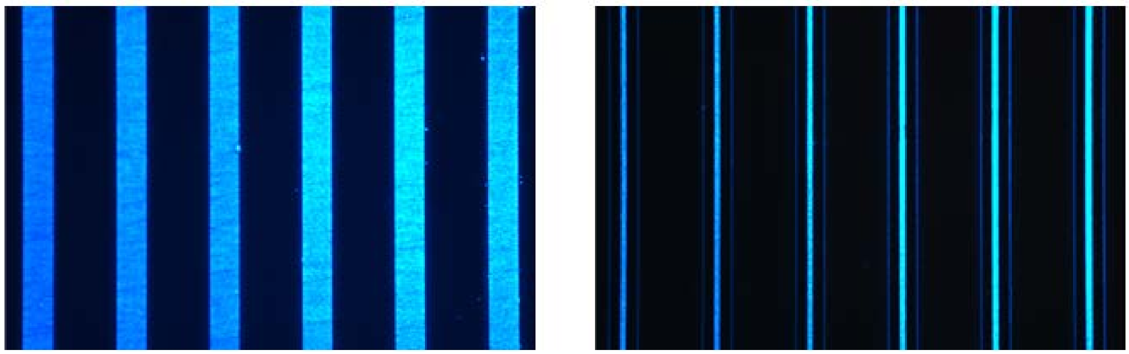

**Figure 20 Flurorescence images of the stripes a) before the PEC-E and without the opaque metal mask on top and b) after the PEC-E with the remaining active region corresponding to the masked area**

As field insulator ~500nm of low temperature SiO2 was deposited on the side of the ridges, followed by the ebeam evaporation of Pd/Au (50nm/1um) layer used as a p-contact. Finally we created the LDs facets by Reactive Ion etching.

Below the several processing steps are summarized.

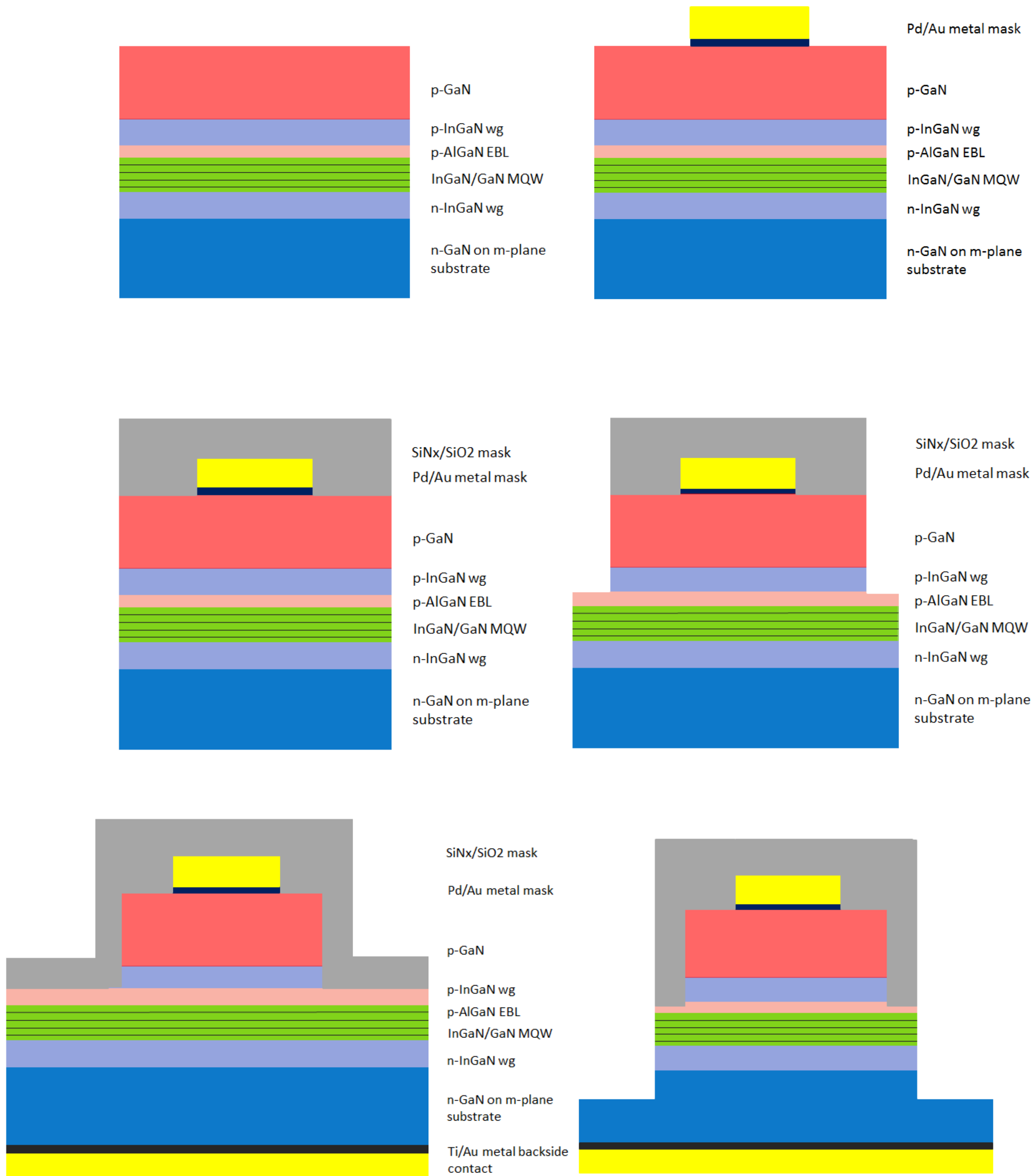

p-GaN
p-InGaN wg
p-AlGaN EBL
InGaN/GaN MQW
n-InGaN wg
n-GaN on m-plane substrate
Pd/Au metal mask
p-GaN
p-InGaN wg
p-AlGaN EBL
InGaN/GaN MQW
n-InGaN wg
n-GaN on m-plane substrate
SiNx/SiO2 mask
Pd/Au metal mask
p-GaN
p-InGaN wg
p-AlGaN EBL
InGaN/GaN MQW
n-InGaN wg
n-GaN on m-plane substrate
SiNx/SiO2 mask
Pd/Au metal mask
p-GaN
p-InGaN wg
p-AlGaN EBL
InGaN/GaN MQW
n-InGaN wg
n-GaN on m-plane substrate
SiNx/SiO2 mask
Pd/Au metal mask
p-GaN
p-InGaN wg
p-AlGaN EBL
InGaN/GaN MQW
n-InGaN wg
n-GaN on m-plane substrate
Ti/Au metal backside contact

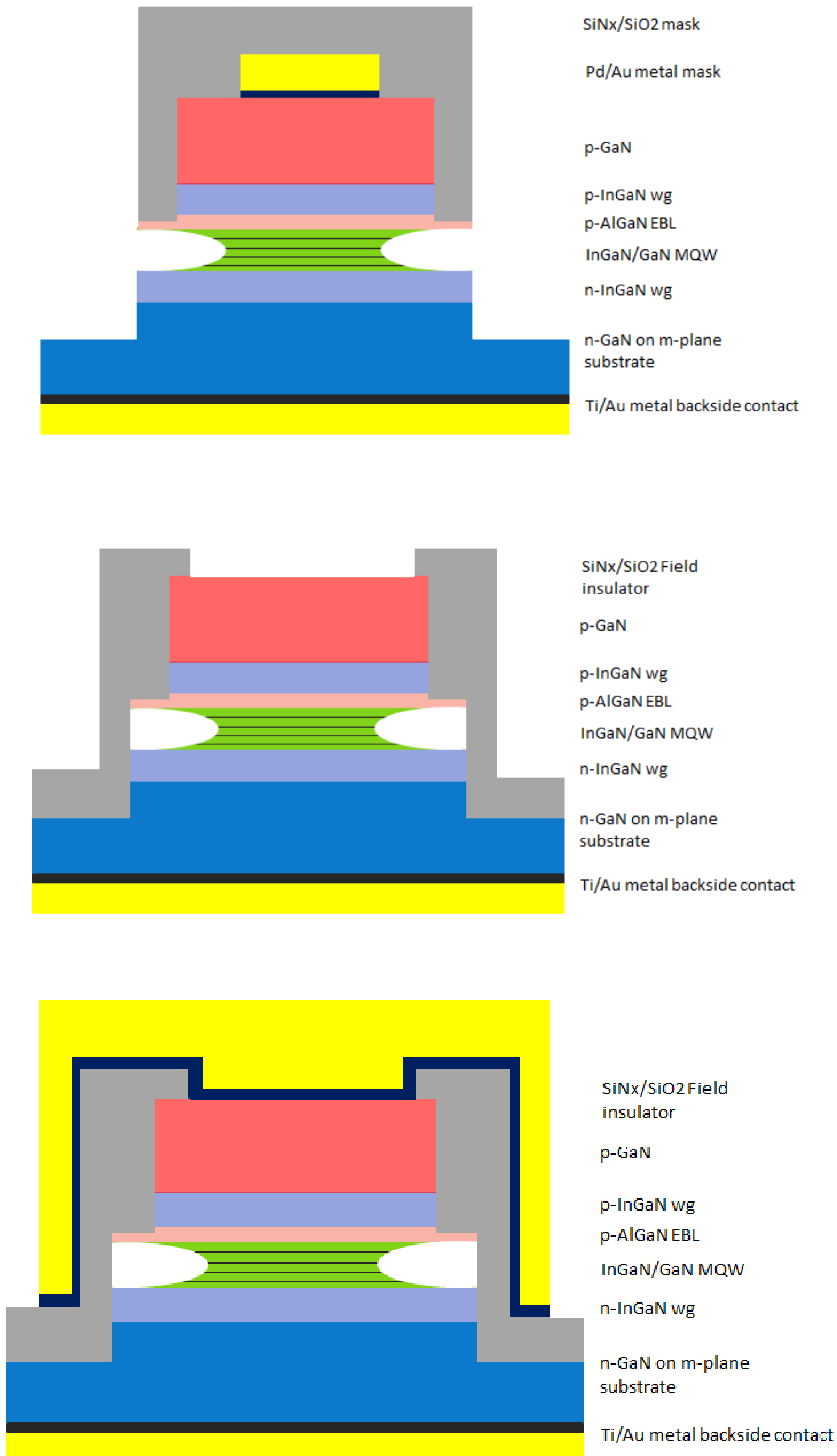


**Figure 21 Process flow of the CA-LD**

In order to to assess the performance of CA-laser, the samples were then cleaved in two pieces, the first was used to fabricate shallow etched ridge LDs using a common edge emitting laser processing which is summarized in Fig. 19, while the second was processed to fabricate the CA-LDs.

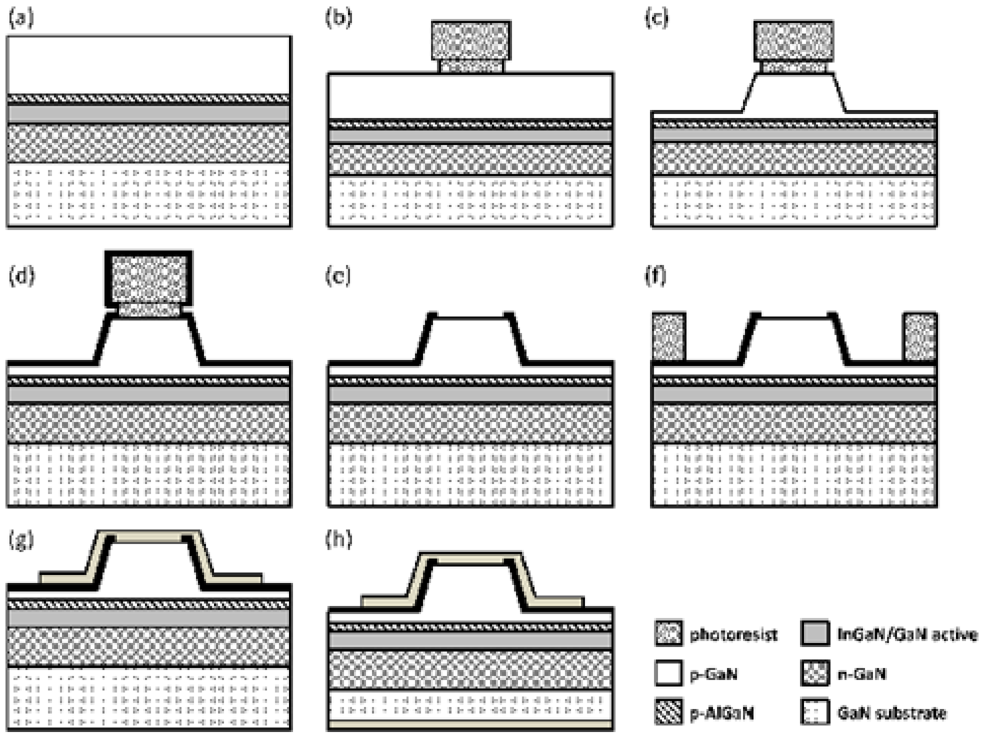


Courtesy to Prof. Feezell, UNM

**Figure 22 Typical process flow of the shallow etched ridge LD**

A schematic of the final structure of both the LDs is depicted in Fig. 23 while Fig. 24 shows a SEM image of the final CA-laser

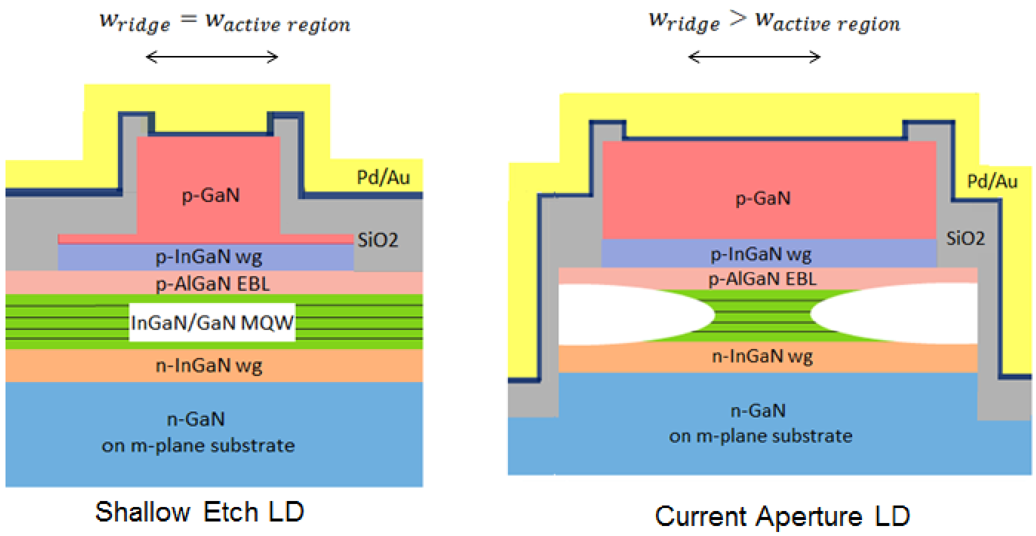


**Figure 23 Schematic cross section of the shallow etched and current aperture deep etched laser structure**

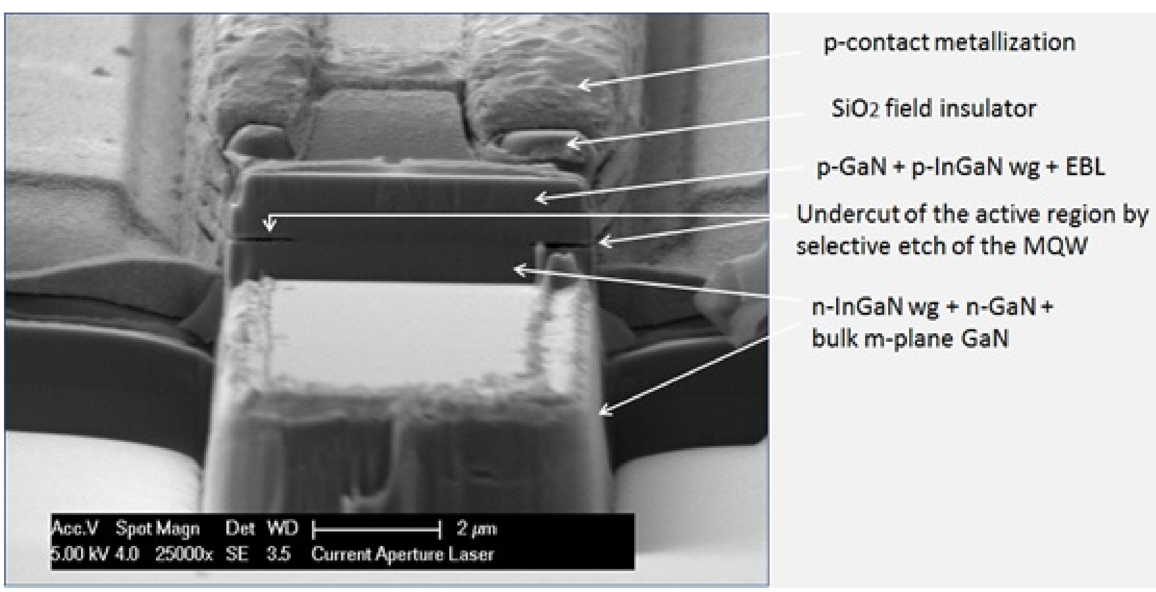


**Figure 24 SEM image of the current aperture deep etched laser fully processed**

### *3.2 CA-Laser Electrical test results*

The devices were tested on-wafer probing under pulsed conditions (pulse width: 300ns, repetition rate: 1kHz, corresponding to a 0.03% duty cycle). The optical output power was measured at room temperature (~22.5 C) from the front facet using a calibrated broad area Si photodetector. The laser facets were not coated.

Fig. shows the IV characteristics for two 1500 um long LDs fabricated according to the two designs. The current aperture LD has a p-GaN ridge width of 10um with an active region width of ~3um after the PECE step, while for the shallow etched LD both the p-GaN ridge and active region width is 3um

Fig. 25 compares the LI characteristics of the two LDs. The threshold current (voltage) are 640mA (16.40V) and 654.7 mA (18.94V) and this corresponds to a threshold current density (Jth) of 14.23 KA/cm2 and 14.55 KA/cm2 for the CA LD and shallow etch LD respectively.

The slope efficiency is 0.069 and 0.017 W/A for the CA-laser and shallow etch LD respectively.

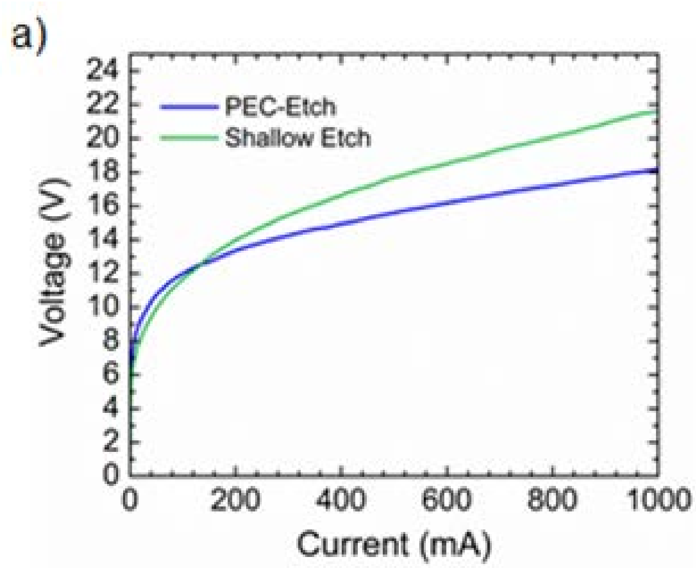

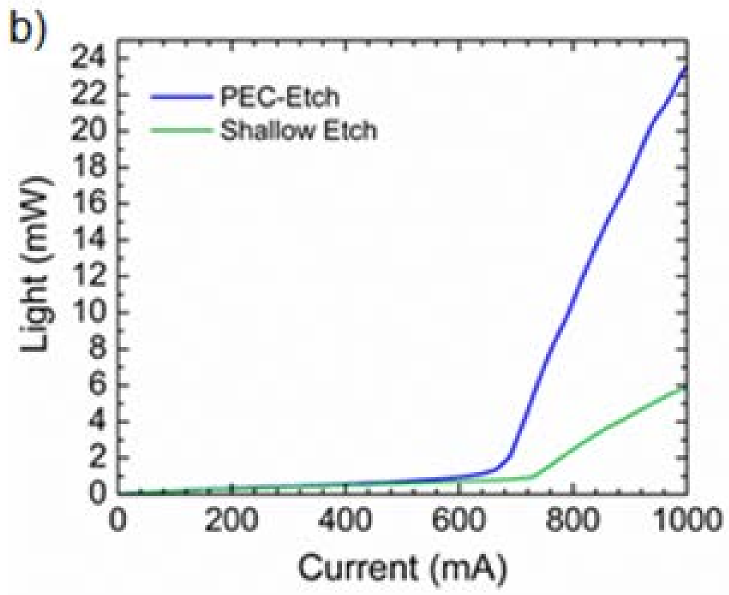


**Figure 25 LIV Characteristics of the PECE and Shallow Etched**

It should be mentioned that the data presented in Fig. 5 is from the best CA-LD and that the aggregate data for the shallow etched ridge LDs has a smaller standard deviation than the aggregate data for the CA-LDs. In general, the threshold current density for other CA-LDs was slightly higher than the threshold current density for shallow etch LDs with an equivalent active area, although the series resistance of the CA-LDs was generally lower. This may be explained in terms of uncompleted PEC-etch of the unmasked active region which results in nanopillar-like structures scattered across the laser bar as shown by the FIB images of Fig. 26 and Fig. 27.

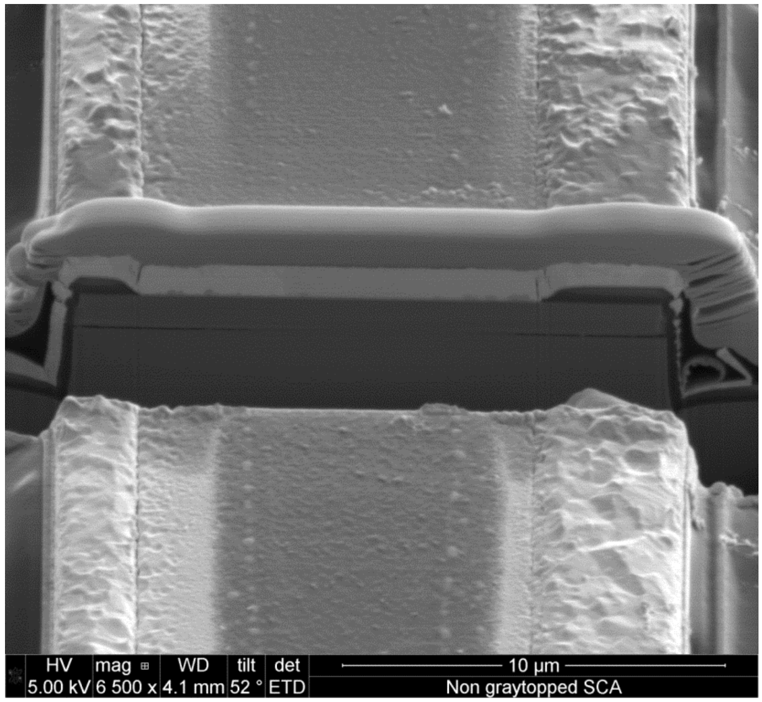


**Figure 26 FIB of a PEC-Etched LD**

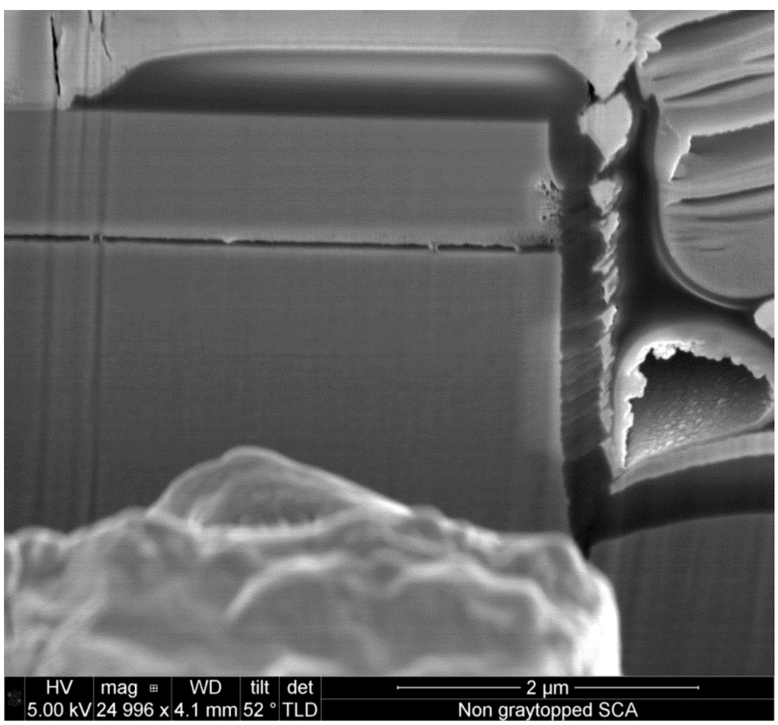


**Figure 27 Detail of FIB of a PEC-Etched LD**

We believe that such nanostructures are located in local highly defective areas of the sample epi-structure where the photo-generated electron/hole pairs tend to recombine immediately and thus the PEC-etching is impeded. Further studies are undergoing by our group to investigate deeper this phenomenon and improve the PEC-etching process.

The relatively high threshold current densities and voltages and relatively low differential efficiencies for both LD designs can be attributed to an unoptimized epitaxial structure and growth conditions and are expected to improve with further development.

In conclusion, we present the first nitride-based current-aperture edge emitting laser by making the top p-GaN area wider than the active region through a selectively PEC-etch of the MQW active layer of laser bars. Control of the PEC-Etching was obtained by blocking the light and the subsequent etching caused by the photo-generated electron/hole pairs using opaque metal masks placed on top of the laser bars. This work demonstrates that the CA-LD has a lower series resistance than the most commonly used shallow etch ridge design for an equivalent active region area. By carefully designing the device geometry and epitaxial structure, the CA-LD may also offer a higher optical confinement factor and lower threshold current density which make this design promising for high-performance, high-power, high-frequency LDs.

## References

[1] S. Nakamura, S.J. Pearton, G. Fasol, *The Blue Laser Diode: The Complete Story*, Springer-Verlag, (2000)

[2] J.J. Wierer Jr., J.Y. Tsao, D.S. Sizov, Laser & Photonics Reviews, **7**, 6, pages 963–993, (2013)

[3] S. Watson, M. Tan, S. P. Najda, P. Perlin, M. Leszczynski, G. Targowski, S. Grzanka, and A.E. Kelly, Optics Letters, **38**, 19, pp. 3792-3794, (2013)

[4] J.W. Raring, M.C. Schmidt, C. Poblenz, Y. Chang, M.J. Mondry, B. Li, J. Iveland, B.Walters, M.R. Krames, R. Craig, P. Rudy, J.S. Speck, S. P. DenBaars, and S.Nakamura, , Appl. Phys. Express 3, 112101, (2010)

[5] J. S. Speck and S. F. Chichibu, *Nonpolar and Semipolar Group III Nitride-Based Materials*, MRS Bulletin, 34: 304-312, (2009)

[6] L.A. Coldren, S.W. Corzine, M. Marshanovitz *Diode Lasers and Photonic Integrated Circuits*, Wiley Series in Microwave and Optical Engineering. (2012)

[7] Md. Satter, P.Yoder, Optical and Quantum Electronics, **42**, 11-13, pp 747-754, (2011)

[8] U. Schwarz, M. Pindl, E. Sturm, M. Furitsch, A. Leber, S. Miller, A. Lell and V. Härle, Phys. Status Solidi A, **202**: 261–270, (2005)

[9] L. Redaelli, H. Wenzel, T. Weig, G. Lükens, S.Einfeldt, U.T. Schwarz, M. Kneissl, and G. Tränkle, J. Appl. Phys. **114**, 113102, (2013)

[10] S. Lutgen, A. Avramescu, T. Lermer, M. Schillgalies, D. Queren, J. Müller, D. Dini, A. Breidenassel, and U. Strauss: Proc. SPIE 7616 (2010)

[11] J.E. Bowers, B.R. Hemenway, A.H. Gnauck, Quantum Electronics, IEEE Journal of, **22**, 6, 833-844, (1986)

[12] M. M. Dummer, J. R. Raring, J. Klamkin, A. Tauke-Pedretti, and L. A. Coldren, OPTICS EXPRESS, **16**, 25, 20388, (2008)

[13] D. Pasquariello, E. S. Björlin, D. Lasaosa, Y. Chiu, J. Piprek, and J. E. Bowers, Journal of Lightwave Technology, **24**, 3, (2006)

[14] J. Daleiden, H. Hillmer, Applied Physics B, **76**, 8, 821-832, (2003)

[15] Y. Cheng, P. Daniel Dapkus, M. H. MacDougal, and G. MO Yang, Photonics Technology Letters, **8**, 2, (1996)

[16] Di Liang, J. Wang, D.C. Hall, Photonics Technology Letters, **19**, 8, 598–600, (2007)

[17] I. Ben-Yaacov, Yee-Kwang; U.K. Mishra, S.P. DenBaars, Journal of Applied Physics, **95**, 4, 2073-2078, (2004)

[18] FIMMWAVE, version 5.4.1, Photon Design (2012)

[19] D. Feezell and S. Nakamura, in Semiconductor lasers: Fundamentals and applications, Edited by A. Baranov and E Tournie, (2013)

[20] A. C. Tamboli, E. D. Haberer, R. Sharma, K. H. Lee, S. Nakamura and E. L. Hu, Nature Photonics **1**, 61–64, (2007)

[21] M. Boroditsky, I. Gontijo, M. Jackson, R. Vrijen, E. Yablonovitch , T. Krauss, C. Cheng, A. Scherer, R. Bhat and M. Krames, J. Appl. Phys. **87**, 3497, (2000)

[22] M. Mosca, A. Castiglia, H.-J. Bühlmann, J. Dorsaz, E. Feltin, J.-F. Carlin and N. Grandjean, Eur. Phys. J. Appl. Phys. **43**, 51-53, (2008)

## Conclusions

This work shows the first Nitride Current Aperture Blue Laser Diode.

The main feature of this LD design consists in making the top p-GaN area wider than the active region through a selectively PEC-etch of the MQWs layer of laser bars. In this way, it is possible to reduce the LD series resistance with respect to the most commonly used shallow etch ridge design for an equivalent active region area and therefore improve the device efficiency. Control of the PEC-Etching was obtained by blocking the light and subsequent photogeneration of electron/hole pairs and etching through opaque metal masks placed on top of the laser bars. By carefully designing the device geometry and epitaxial structure, the CA-LD may also offer a higher optical confinement factor and lower threshold current density which make this design promising for high-performance, high-power, high-frequency LDs.